

https://doi.org/10.1093/cercor/bhac118 Original Article

# Signals from posterior parietal area 5 to motor cortex during locomotion

Irina N. Beloozerova [D, PhD1,2,\*, Wijitha U. Nilaweera, PhD2,3, Gonzalo Viana Di Prisco, PhD2,4, Vladimir Marlinski, PhD2

- <sup>1</sup>School of Biological Sciences, Georgia Institute of Technology, 555 14th Street, Atlanta, GA, 30332, USA,
- <sup>2</sup>Barrow Neurological Institute, St. Joseph's Hospital and Medical Center, 350 West Thomas Road, Phoenix, AZ, 85013, USA,
- <sup>3</sup>Des Moines Area Community College, 2006 South Ankeny Blvd., Ankeny, IA, 50023, USA,
- <sup>4</sup>Stark Neurosciences Research Institute, Indiana University, 320 West 15th Street, Indianapolis, IN, 46202, USA
- \*Corresponding author: School of Biological Sciences, Georgia Institute of Technology, 555 14th Street, Atlanta, GA, 30332, USA. Email: ibeloozerova3@gatech.edu

#### **Abstract**

Area 5 of the parietal cortex is part of the "dorsal stream" cortical pathway which processes visual information for action. The signals that area 5 ultimately conveys to motor cortex, the main area providing output to the spinal cord, are unknown. We analyzed area 5 neuronal activity during vision-independent locomotion on a flat surface and vision-dependent locomotion on a horizontal ladder in cats focusing on corticocortical neurons (CCs) projecting to motor cortex from the upper and deeper cortical layers and compared it to that of neighboring unidentified neurons (noIDs). We found that upon transition from vision-independent to vision-dependent locomotion, the low discharge of CCs in layer V doubled and the proportion of cells with 2 bursts per stride tended to increase. In layer V, the group of 2-bursters developed 2 activity peaks that coincided with peaks of gaze shifts along the surface away from the animal, described previously. One-bursters and either subpopulation in supragranular layers did not transmit any clear unified stride-related signal to the motor cortex. Most CC group activities did not mirror those of their noID counterparts. CCs with receptive fields on the shoulder, elbow, or wrist/paw discharged in opposite phases with the respective groups of pyramidal tract neurons of motor cortex, the cortico-spinal cells.

Key words: cat; cortical layer; somatosensory; vision; walking.

## Introduction

Area 5 of the posterior parietal cortex receives both visual- and movement-related information and is involved in the control of limb movements (reviewed in Mountcastle 1995; Andersen et al. 1997; Andersen and Cui 2009; Gamberini et al. 2020). Lesions in this area cause optic ataxia, i.e. the inability to accurately direct limbs to visual targets (Rondot et al. 1977; Fabre and Buser 1980, 1981; Hyvarinen 1982; Ungerleider and Mishkin 1982; Batuev et al. 1983). This includes the inability to accurately step over obstacles on the pathway (Lajoie and Drew 2007; Wong, Pearson, et al. 2018; Wong, Wong, et al. 2018). During locomotion, the activity of neurons in area 5 is modulated with the rhythm of strides (Beloozerova and Sirota 1992, 2003; Andujar et al. 2010). It reflects visual heterogeneity of the walking surface (Beloozerova and Sirota 2003) and the distance and time to contact with an obstacle (Marigold and Drew 2017). On a complex terrain, this activity is suggested to contribute to the planning of visually guided gait modifications (Andujar et al. 2010; Wong and Lomber 2019) and interlimb coordination (Lajoie et al. 2010). However, how the activity of area 5 contributes to adjusting strides on the complex terrain is not fully understood.

Axons of many area 5 neurons descend within the pyramidal tract and synapse on spinal interneurons (Groos et al. 1978; Asanuma 1981; Murray and Coulter 1981; Wiesendanger 1981; Hyvarinen 1982; Rathelot et al. 2017). Thus, the activity of area 5 can contribute to the adjustment of strides by influencing the locomotionrelated circuitry of the spinal cord. However, area 5 also intensively projects to other brain areas involved in the control of movements, such as motor and premotor cortex (Strick and Kim 1978; Hyvarinen 1982; Waters et al. 1982; Babb et al. 1984; Yumiya and Ghez 1984; Kakei et al. 1996; Ghosh 1997b; Andujar and Drew 2007), basal ganglia, superior colliculus, and pontine nuclei (Wiesendanger et al. 1979; Hyvarinen 1982; Leichnetz et al. 1984). Therefore, one can expect that in addition to directly modulating the locomotor circuitry of the spinal cord, area 5 also influences it indirectly via projections to other motor centers of the brain. Indeed, the posterior parietal area 5 is considered to be a part of the cortical "dorsal stream," the "Where?" pathway, a cortical pathway that processes visual information for action and conveys it from visual cortex in the occipital lobe to cortical motor areas in front of the brain, thereby equipping them with processed visual information

for guiding limbs to objects (Ungerleider and Mishkin 1982; Goodale and Milner 1992; Gallivan and Goodale 2018). While the transmission of information between cortical areas at the beginning of the dorsal stream was investigated in a number of studies (e.g. Sherk 1989, 1990), the signals that the posterior parietal area 5 ultimately conveys to motor cortex remained unknown. This hampers understanding of the contribution of area 5 to the control of locomotion and movements in general and leaves the question of how the activity of motor cortex depends on information arriving via the cortical dorsal stream open.

In this study conducted on cats walking freely on surfaces that do or do not require visual control of steps, we recorded the activity of area 5 neurons projecting to motor cortex from different cortical layers and compared it with the activity of general area 5 populations in the respective layers. The goal was to understand what movement- and vision-related information area 5 conveys to motor cortex during vision-independent and vision-dependent locomotion. In the Results section, we first characterize the studied neuronal populations, including their activity at rest. We then describe the locomotion-related activity of the two major groups of neurons that fire 1 burst or 2 bursts per step cycle while looking at how they shape the activity of the upper and deeper cortical layers and the signals to motor cortex originating in these layers. Finally, we compare the activity of groups of neurons related to different segments of the forelimb to unveil the signals that they transmit to networks that govern movements of different forelimb segments. In the Discussion, we correlate the group activity of the key area 5 subpopulations with the gaze behavior of these cats described previously (Zubair et al. 2019) to evaluate visual information that may reach motor cortex via area 5 during different phases of the stride.

# **Methods** Experimental strategy

The experiments were conducted on cats because the activity of the general area 5 population during locomotion in cats has been described (e.g. Beloozerova and Sirota 2003; Andujar et al. 2010; Lajoie et al. 2010; Marigold and Drew 2011, 2017) as was the activity of motor cortex (e.g. Armstrong and Drew, 1984a, 1984b; Drew 1988, 1993; Beloozerova and Sirota, 1985, 1993a, 1993b; Beloozerova et al. 2010; Stout and Beloozerova 2012, 2013; Farrell et al. 2014, 2015). This made it easier to evaluate how signals from area 5 may influence the motor cortex activity. Cats walked on a flat surface, a task that does not require vision, and along a horizontally placed ladder, a task that requires vision, which allowed us to study transmission of both movement-related and vision-related signals from area 5 to motor cortex. These signals were assessed using single neuron recordings from area 5 cells projecting an axon to motor cortex,

corticocortical neurons (CCs). These neurons were identified in walking animals using a test of collision of spontaneous spikes with the spikes evoked by electrical stimulation in motor cortex (Bishop et al. 1962; Fuller and Schlag 1976; also, e.g. Stout and Beloozerova 2013). Neurons were grouped according to the pattern of the discharge during the step cycle, cortical layer position of their somata, and receptive field (RF). The activity profile of each group was compared between the two locomotion tasks to determine the movement- and vision-related components of the activity. Within each category, the groups were compared to determine the role of the discharge pattern, cortical layer, and RF.

The experimental protocol was in compliance with the National Institutes of Health guidelines for the care and use of laboratory animals and was approved by the Barrow Neurological Institute Animal Care and Use Committee.

#### **Animals**

Extracellular recordings from single neurons in the posterior parietal cortex area 5 were obtained during chronic experiments in 2 adult cats, a female (cat 1, weight: 3.7 kg) and a male (cat 2, weight: 4.0 kg). Cats were purchased from a certified commercial class B dealer. The methods of surgical preparation and recording techniques have been described in detail previously (Prilutsky et al. 2005) and will be only briefly reported here. Data on the activity of motor and somatosensory cortex and the thalamus during locomotion obtained from these cats were included in previous publications: on motor cortex in Beloozerova et al. (2010) (cat 1), Armer et al. (2013) (cat 2), Stout and Beloozerova (2013) (cat 2), and Farrell et al. (2014, 2015) (cat 1); on somatosensory cortex in Favorov et al. (2015) (cat 1); and on the thalamus in Marlinski, Nilaweera, et al. (2012) (cat 2), Marlinski, Sirota, et al. (2012) (cat 1), and Marlinski and Beloozerova (2014) (cat 1). In addition, data on the movement of the head and gaze during locomotion collected from these cats were reported in Rivers et al. 2014 (cats 1 and 2) and Zubair et al. 2016, 2019 (cats 1 and 2).

#### Locomotion tasks

Two tasks were used: locomotion on a flat surface, and locomotion on crosspieces of a horizontally placed ladder (Fig. 1A). It has been demonstrated in several studies that locomotion on the flat surface does not require vision and can be accomplished without the forebrain, while accurate stepping on a complex surface, such as the ladder, relies on vision and participation of the cortex (Trendelenburg 1911; Liddell and Phillips 1944; Chambers and Liu 1957; Beloozerova and Sirota 1988, 1993a, 2003; Metz and Whishaw 2002; Farr et al. 2006; Friel et al. 2007). Thus, the neuronal activity during locomotion on the flat surface is primarily related to the locomotor movement, whereas that during vision-guided stepping on the ladder represents a combination of the activity related to (i) the locomotor movement and (ii) processing of visual

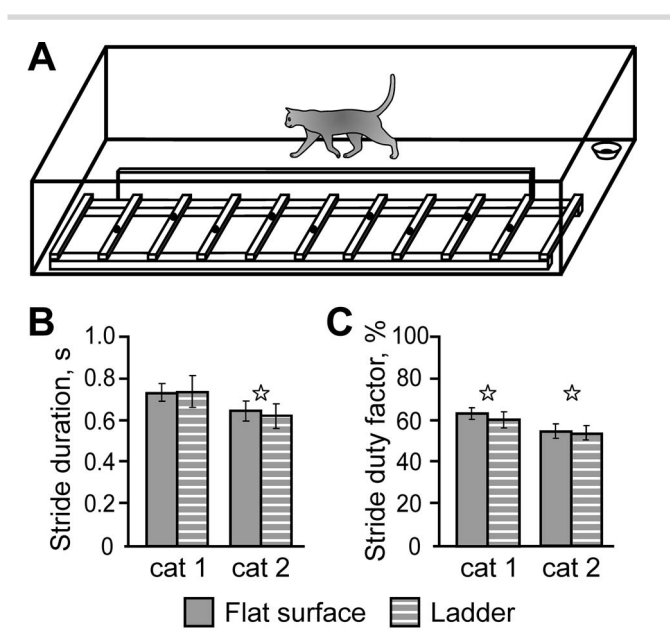


Fig. 1. Locomotor tasks. A) The experimental box was divided into two corridors. In one corridor, the floor was flat, whereas the other corridor contained a horizontal ladder. Cats walked at a self-selected speed. Filled circles on the crosspieces of the ladder schematically show placements of the right and left paws. B) Duration of strides during flat surface and ladder locomotion. C) Stride duty factor (proportion of the stance phase in the step cycle) during flat surface and ladder locomotion. In B, C), error bars show SDs, stars indicate statistically significant difference between locomotion tasks (P < 0.05, t test).

information required for accurate stepping on the ladder. When the biomechanics of the locomotor movement on the ladder are similar to those on the flat surface, the vision-related component can be isolated by comparing the neuronal activity during ladder locomotion to that on the flat surface (e.g. Beloozerova and Sirota 1988, 1993a, 2003; Beloozerova et al. 2010; Favorov et al. 2015; Beloozerova and Marlinski 2020). We have shown that when crosspieces of a ladder are at a distance of the cat's normal step length and have flat tops wide enough to provide full support for the paw, the biomechanics of ladder locomotion are close to those on the flat surface (Beloozerova et al. 2010). Thus, comparing neuronal activity during vision-dependent locomotion on such a convenient ladder with that during vision-independent locomotion on the flat surface allowed us to distinguish parts of neuronal activity related to the processing of visual information required for the accurate stepping on the ladder and those related to locomotor movement itself.

Positive reinforcement by food was used to adapt cats to the experimental situation and to engage them in locomotion (Skinner 1938; Pryor 1975). Cats were trained to walk in an experimental chamber that was a rectangular enclosure with two connected parallel corridors 2.5 × 0.3 m each. In one corridor, the floor was flat, while the other corridor contained the horizontal ladder. The centers of the ladder crosspieces were spaced 25 cm apart, equal to 1/2 of the cat's average stride length during locomotion in the chamber with the flat floor (Beloozerova and Sirota 1993a; Beloozerova et al. 2010). The crosspieces had

flat tops 5 cm wide, which was slightly greater than the 3 cm diameter support area of the cat's paw (e.g. de Carvalho et al. 2015). During walking on the ladder, each limb overstepped two gaps and every other crosspiece of the ladder (Fig. 1A). While going around the chamber, cats passed through the two corridors sequentially and repeatedly, occasionally changing direction from clockwise to counterclockwise. After each round, food was dispensed into a feeding dish in one of the corners. Cats were trained, upon arrival, to stand in front of the feeding dish quietly for 3-5 s. One second in the middle of this period was considered as "standing."

Cats were accustomed to wearing a cotton jacket, a light backpack with electrical connectors and a sock on the right forelimb paw with a small metal plate on the sole for recording paw contact with the floor and the ladder's crosspieces. The floor in the chamber and the crosspieces of the ladder were covered with an electrically conductive rubberized material. The duration of the swing and stance phases of the stride of the right forelimb, which is contralateral to the left cortex where the activity of neurons was recorded (see below), was monitored by measuring the electrical resistance between the plate and the floor. We refer to the full movement cycle of one limb (from the beginning of a swing to the beginning of the next swing of the same limb) as a step cycle or stride and use these terms interchangeably.

# Surgical procedures

Surgery was performed under Isoflurane anesthesia using aseptic procedures. The skin and fascia were retracted from the dorsal surface of the skull, and at 10 points around the circumference of the skull, stainless steel screws were implanted. The screw heads were then embedded into a plastic cast to form a circular base. Later, this base was used for fixating electrical connectors, electrode microdrives, preamplifiers, and to rigidly hold the cat's head while searching for neurons.

On the left side of the head, the dorsal surface of the posterior parietal cortex in the rostral suprasylvian and lateral gyri and the dorsal surface of motor cortex in the anterior, posterior, and lateral sigmoid gyri were exposed by removing approximately 1.4 cm<sup>2</sup> of bone and dura mater. The regions of the rostral part of the posterior parietal cortex and motor cortex in the pericruciate cortex were visually identified based on surface features and photographed (Figs. 2A–D and 3A). The exposure was covered with a 1-mm thick acrylic plate. The plate was preperforated with holes of 0.36 mm in diameter which were spaced by 0.5 mm; the holes were filled with a bone wax and petroleum jelly mixture. This plate allowed access to the cortex in the awake animal for recording and stimulation. Later, in the awake cat, several 140- $\mu$ m platinum-iridium wires (A-M Systems, Carlsborg, WA) insulated with teflon to within 0.4 mm of the tapered tip were inserted through these openings into motor cortex after its physiological mapping to serve as stimulation electrodes for antidromic identification

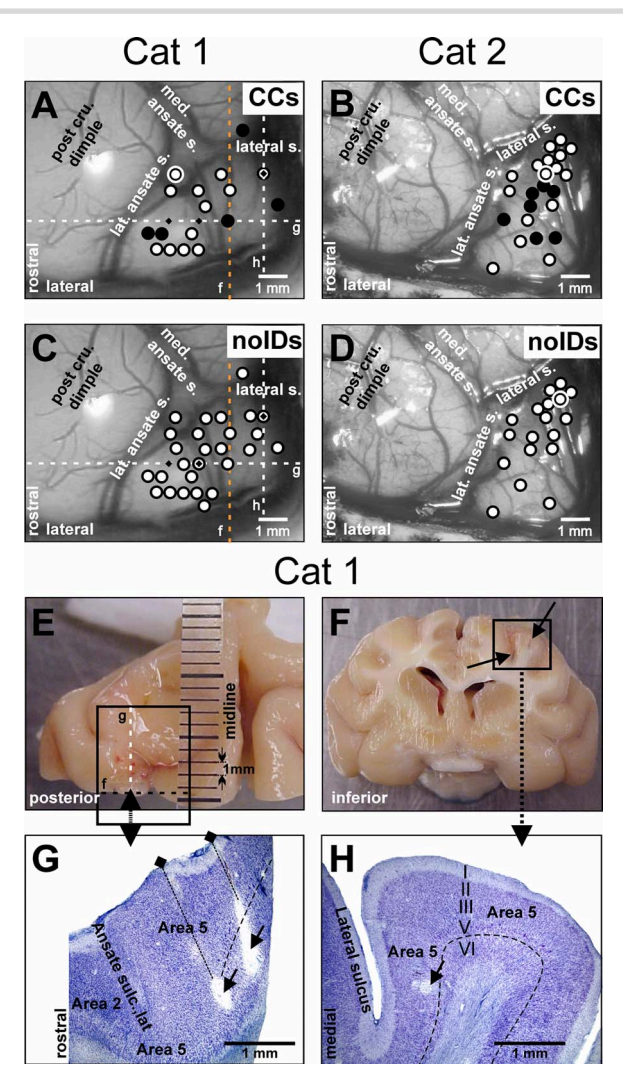


Fig. 2. Area of recording in the rostral part of the suprasylvian gyrus. A-D) The top view of the live cortex of cat 1 (A, C) and cat 2 (B, D). Microelectrode entry points into the cortex are shown by circles. A, B) Microelectrode entry points of tracks from which the activity of neurons with an axon projecting to ipsilateral motor cortex (CCs) was recorded. Open circles show tracks from which the activity of CCs was recorded during locomotion; filled circles show those where CCs were identified and their activity during sitting but not walking was recorded. In A), the microelectrode track is highlighted by a white ring from where the neuron was recorded, the antidromic responses of which to electrical stimulation of motor cortex are shown in Fig. 3B. In B), the microelectrode track is highlighted by a white ring from where the neuron was recorded, the activity of which during locomotion is shown in Fig. 5F-J. C, D) Microelectrode entry points of tracks from where neurons with an unknown projection of the axon, as well as several neurons with an axon descending to the midbrain (cat 1 only) or descending within the medullar pyramidal tract, were collected. This group of neurons is collectively referred to as nonidentified neurons (noIDs). In cat 1, noIDs were recorded from all 17 microelectrode tracks, from which CCs were recorded, as well as from 10 additional tracks that were immediately adjacent. In cat 2, noIDs were recorded from all but 2 microelectrode tracks, from which CCs were recorded during locomotion, and from 4 of 7 tracks, in which CCs were identified but their activity was only recorded in the sitting animal. In D), the microelectrode track is highlighted by a white ring from where the neuron was recorded, the activity of which during locomotion is illustrated in Fig. 5A-E. In A, C), horizontal dashed line g indicates the position of the parasagittal section shown in G), and black diamonds show the cortical entry points of electrode tracks where the reference lesions were made. Vertical orange dashed line f indicates the line along which the brain of cat 1 was cut into the frontal and caudal blocks; these blocks are shown in E, F), respectively. Vertical white dashed line h indicates the position of the frontal section shown in H, and the black diamond specifies the cortical entry point of the electrode track

of posterior parietal cortex neurons projecting to motor cortex (see details below).

In addition, to identify area 5 neurons with axons descending within the pyramidal tract, two 26-gage hypodermic guide tubes fitted with stainless steel wires were implanted 7 mm above the left medullary pyramidal tract, placed 1 mm apart in the rostro-caudal direction. Later, in the awake cat, a 200-µm platinumiridium wire insulated with teflon to within 0.4 mm of the tapered tip was inserted into the medullary pyramid using physiological guidance (Prilutsky et al. 2005) to serve as a stimulation electrode. In cat 1, an arrangement of seven 28-gage hypodermic guide tube was implanted above the left brachium of the superior colliculus and rostro-lateral part of the left red nucleus, and stimulation electrodes were inserted there after physiological mapping of the areas in the awake animal for identification of axonal projections of area 5 neurons to the midbrain. Immediately after the surgery, and 12 h thereafter, an analgesic buprenorphine was administered subcutaneously.

## Single-unit recording and neuron identification in the posterior parietal cortex

Extracellular recordings of single neuron activity were obtained from the rostral part of the suprasylvian gyrus (Fig. 2A and B). This area in cats is considered to be the forelimb-related posterior parietal cortex area 5 based on data from histological examination, inactivation, and activity recording (Hassler and Muhs-Clement 1964; Waters et al. 1982, Avendano et al. 1985, 1988; Beloozerova and Sirota 2003; Lajoie and Drew 2007; Andujar and Drew 2007; Andujar et al. 2010; Lajoie et al. 2010; Wong, Pearson, et al. 2018; Wong, Wong, et al. 2018). The area of recordings covered a smaller region of the cortex compared to that studied in our earlier work (Beloozerova and Sirota 2003).

Tungsten varnish-insulated microelectrodes (120  $\mu$ m; FHC Inc., Bowdoin, ME) or platinum-tungsten quartz insulated microelectrodes (40  $\mu$ m) were used to record electrical activity of neurons (impedance: 1-3 M $\Omega$  at 1,000 Hz). A lightweight (2.5 g) manual single-axis micromanipulator permanently mounted on the cat's head was used to advance the microelectrode. Signals from the microelectrode were preamplified with a preamplifier on the cat's head and were further amplified and filtered (0.3–10 kHz band-pass) with the CyberAmp 380 (Axon Instruments). After amplification, signals were digitized with a sampling frequency of 30 kHz and were recorded using a data acquisition and analysis package (Power1401/Spike2 System, Cambridge Electronic Design, Cambridge, UK). The Power1401/Spike2 waveformmatching algorithm was used to initially identify and isolate spikes of single neurons. Only well-isolated neurons were used for further analyses.

For identification of area 5 neurons that project an axon to the ipsilateral motor cortex (CCs), stimulating electrodes were implanted into the representation of the distal forelimb (wrist and paw, MCdist) and proximal forelimb (shoulder and elbow, MCprox) in the area 4y of motor cortex and, in cat 1, also into the adjacent area 6 ( $6a\alpha$  and 6iffu, Ghosh 1997a) of the premotor cortex (Fig. 3A). In cats, the cortex on the surface of the lateral sigmoid (sig. l.) and the lateral part of the anterior sigmoid (sig. a.) gyri is considered to be the forelimb-related motor cortex based on data obtained using inactivation, stimulation, and recording techniques (Nieoullon and Rispal-Padel 1976; Phillips and Porter 1977; Vicario et al. 1983; Armstrong and Drew 1984c, 1985; Martin and Ghez 1993; Beloozerova and Sirota 1993a; Beloozerova et al. 2010; Stout and Beloozerova 2012, 2013; Farrell et al. 2014, 2015). Since the exact location of the regions related to the distal and proximal forelimb slightly varies among subjects, their positions in each cat were identified using multiple-unit mapping procedures before stimulating electrodes were implanted. Furthermore, the locomotion-related activity of the so-identified motor cortex area was analyzed and reported for cat 1 in Beloozerova et al. (2010) and Farrell et al. (2014, 2015) and for cat 2 in Armer et al. (2013) and Stout and Beloozerova (2013).

Area 5 neurons with axons descending within the pyramidal tract, pyramidal tract projection neurons (PTNs), were identified by their antidromic responses to electrical stimulation of the pyramidal tract at the medulla level through an electrode implanted there as described above. In cat 1, area 5 neurons sending axons to the rostral part of the ipsilateral red nucleus and the ipsilateral pretectal area and brachium of the superior colliculus in the midbrain were identified by their antidromic responses to the electrical stimulation of these areas via electrodes implanted there.

All neurons encountered in tracks through area 5 were tested for antidromic activation using 0.2-ms rectangular pulses of graded intensity in the range of 0.1-2 mA, with currents for stimulation of the pyramidal tract limited to 0.5 mA. The principal criterion for identification of antidromic activation was the test for the collision of spontaneous and evoked spikes (Bishop et al. 1962; Fuller and Schlag 1976; see also e.g. Beloozerova et al. 2003; Stout and Beloozerova 2013). The collision test is illustrated in Fig. 3B and is explained in the legend to the figure. In addition, silent neurons that could not be tested

for the collision of spikes for the lack of spontaneous activity were considered to be antidromically activated if they satisfied two ancillary criteria: (i) a refractory period of <2.0 ms and (ii) latency variability to a test stimulus of either <0.1 ms or <1% of the antidromic latency, whichever is greater when the test stimulus follows a suprathreshold conditioning stimulus at an interval of 10 ms (Swadlow et al. 1978). To discover silent neurons, one pulse of electrical stimulation was applied through each stimulating electrode for each 50  $\mu$ m advancement of the recording electrode. Each recorded neuron was tested for antidromic activation before, during, and after every locomotion test.

For calculation of the axonal conduction velocity, the distances from the recording electrode in the rostral part of the suprasylvian gyrus and the stimulation electrodes were estimated as follows: to MCdist, 9-12 mm (cat 1, depending on the location in area 5; Fig. 3A), 15 mm (cat 2); to MCprox, 11-14 mm (cat 1), 16 mm (cat 2); and to area 6 adjacent to MCprox ( $6a\alpha$  and 6iffu), 12–15 mm (cat

Cortical layer V was identified by the presence of PTNs. PTNs and neurons recorded in-between PTNs or within 100  $\mu$ m of the first or last PTN along a microelectrode track were considered located in layer V. Neurons recorded 100  $\mu$ m or more above the first identified PTN were considered to be in layers II-IV. Neurons recorded 100  $\mu$ m or more below the last identified PTN along a microelectrode track were considered to be in layer VI. In tracks where no PTNs were identified, the depth of layer V was inferred based on data from the neighboring

The nonidentified neurons (noIDs) in this study were the cells that did not respond antidromically to electrical stimulation of the forelimb representation in the lateral aspect of the ipsilateral anterior sigmoid gyrus or the lateral sigmoid gyrus, although they might have projected to the forelimb representation in motor cortex because the size of this representation in the cat is much larger than that estimated to be excited by the current from the stimulation electrodes that we used (Hentall et al. 1984; Swadlow 1998). The noIDs included PTNs, neurons responding antidromically to electrical stimulation of the midbrain, and neurons that did not respond antidromically to stimulation through any

where the reference lesion was made. E, F) Postmortem blocks of cat 1 brain showing marks left by reference electrodes (E) and reference stain deposits (F). E) Top view at the rostral block. The area of the cortex shown in A, C) is outlined by the black rectangle, lines f and g are shown. Red marks near the posterior end of the block left by reference electrodes are visible above the arrow. F) The rostral cut of the caudal block immediately adjacent to the rostral block shown in E). The black square approximately outlines the area of the section shown in H). Arrows point to black ink deposits that were introduced during the terminal experiment for reference. G) Photomicrograph of a parasagittal section from the rostral block shown in E. The level of the section is indicated by an arrow in E and the horizontal dashed line g in A and C. Arrows point to reference lesions made in the area of recordings during the terminal experiment. Black diamonds show entry points into the cortex of the electrode that was used to make the lesions, and the dotted lines highlight the tracks. Note that the tracks were made perpendicular to the cortical surface, which raises up as it goes from the front to the middle of the hemisphere. Layer V, which contains giant pyramidal cells characteristic for area 5, is highlighted by a dashed line drawn below it in the area of the lesions. H) Photomicrograph of a frontal section from the caudal block shown in F. The area of the section shown is approximately outlined in F by a black square. Vertical white dashed line h in A and C indicates the position of the section. The arrow points to a reference lesion in the area of recordings in the lateral bank of the Lateral sulcus. The black diamond on line h in A and C shows the cortical entry point of the electrode that was used to make the lesion. Layers of the cortex are numbered. Layer V, which contains giant pyramidal cells characteristics of area 5, is highlighted by a dashed line drawn below it. G, H) Cresyl violet stain.

stimulation electrodes implanted in the animal. Thus, the noIDs of this study included a diverse mix of interneurons and various efferent neurons.

The somatosensory RFs of the neurons were examined in animals sitting with restrained head. Stimulation was produced by lightly stroking fur, palpation of the muscle bellies and tendons, and passive movements around limb joints. Neurons that had somatosensory RFs on the forelimb, neck, or face were included in the analyses. Several neurons recorded from cat 2 that had somatosensory RFs on the hindlimb were excluded.

Responses to visual stimulation were tested by presenting moving 3D stimuli, such as toys, laboratory objects, and hands, to the sitting cat. Such stimuli are known to be most effective at evoking responses of posterior parietal cortex neurons (e.g. Hyvarinen 1982). The stimuli were presented against the natural laboratory background and were moved in different directions in the frontal plane at a distance of  $\sim$ 50 cm in front of the animal and also toward the animal and away from it at a speed of 0.5-1.0 m/s.

In summary, individual neurons were identified according to: (i) location in the rostral suprasylvian gyrus; (ii) cortical layer position of their somata, which in this study was recognized as either being above layer V (layers II-IV), layer V, or layer VI; (iii) projection to the forelimb representation in the ipsilateral motor cortex, the distal or proximal limb-related; (iv) the axonal conduction velocity; (v) somatosensory RF; and (vi) visual RF.

## Processing of neuronal activity

From the 4 or 5 strides that the cat took along each corridor (Fig. 1A), 2 strides in the middle were selected for analysis. The strides were further selected so that their average duration during flat surface and ladder locomotion in each session differed by no more than 10%. Selecting strides of similar duration minimized potential differences in the activity of neurons due to the difference in the speed of locomotion during the two tasks. Each group of selected strides contained at least 15 strides.

The onset of the swing phase of the right forelimb was taken as the beginning of the step cycle. The step cycles were time-normalized, and raster plots were created to visualize the discharge of the neurons over all selected step cycles (e.g. Fig. 5B and D). The duration of each step cycle was divided into 20 equal bins, and for neurons that discharged at least 2 spikes during a task, a phase histogram of the discharge rate during the cycle was generated and averaged over all selected cycles (e.g. Fig. 5C and E). The phase histogram was smoothed by recalculating the value of each bin as follows:  $F_n' = 0.25F_{n-1} + 0.5F_n + 0.25F_{n+1}$ , where  $F_n$  is the original value of a bin. A coefficient of the striderelated activity modulation, the "depth" of modulation (dM), was calculated as dM = (Nmax - Nmin)/N \* 100%,

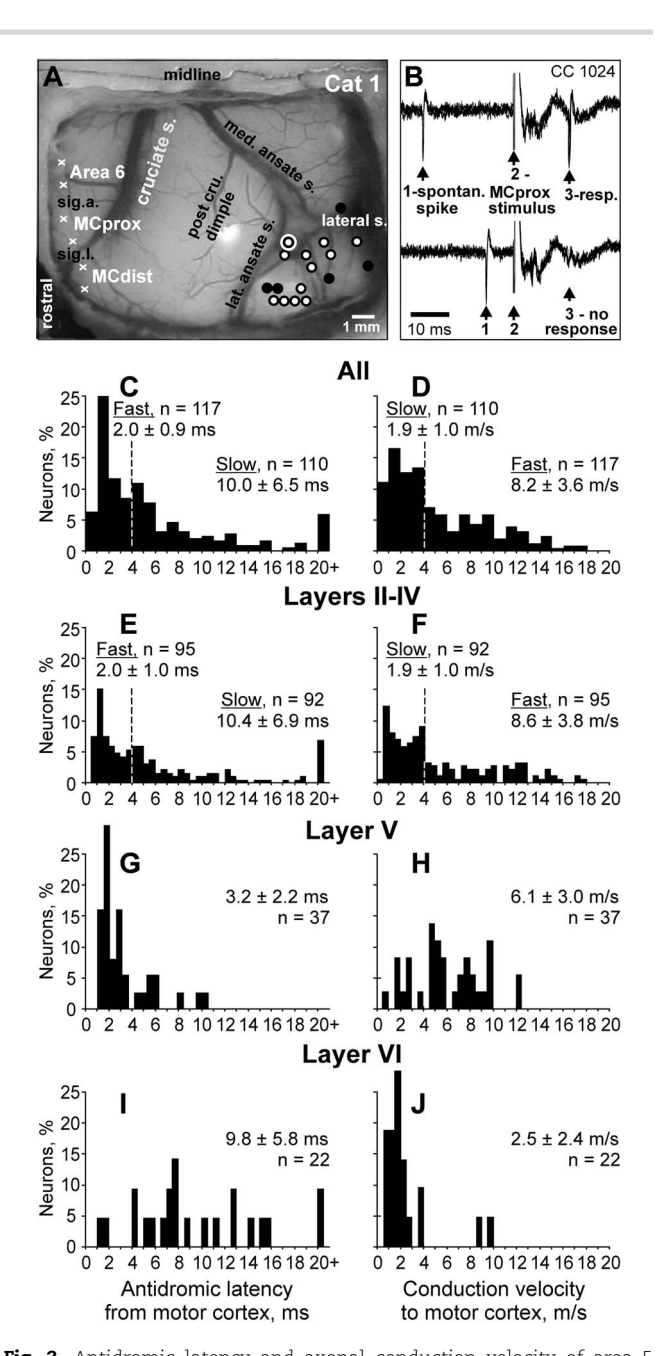


Fig. 3. Antidromic latency and axonal conduction velocity of area 5 neurons projecting to the ipsilateral motor cortex, CCs. A) Photograph of the dorsal surface of the left frontal cortex of cat 1 (zoom-out on the image shown in Fig. 2A). Microelectrode entry points into the rostral part of the suprasylvian gyrus, from which CCs were recorded, are shown by circles as in Fig. 2A. Entrance points of stimulation electrodes into the lateral sigmoid (sig. l.) and the lateral part of the anterior sigmoid (sig. a.) gyri are shown by white crosses. Electrodes were placed in the wrist- and paw-related area of motor cortex (the distal forelimb representation, MCdist) and across the shoulder- and elbow- related areas (the proximal forelimb representation, MCprox) as determined by recording and microstimulation procedures. In cat 1, electrodes were also implanted in the adjacent area 6 of the premotor cortex (area 6) as determined by postmortem histological examination of the tissue. Entrance points of stimulation electrodes into the precruciate gyrus of cat 2 can be seen on a photograph of the dorsal surface of the left frontal cortex of this cat shown in Figure 5A in Marlinski, Nilaweera, et al. (2012). B) Illustration of the collision test. Top trace, the CC #1024 spontaneously discharged (arrow 1) and MCprox was stimulated 24 ms later (arrow 2). The CC responded with a latency of 14.4 ms (arrow 3). Five sweeps are superimposed. Bottom trace, the CC spontaneously

where Nmax and Nmin are the numbers of spikes in the maximal and minimal histogram bin, and N is the total number of spikes in the histogram. The activity with dM > 4% was judged to be stride-related. This threshold was adopted to be the same as that for the activity of neurons in the cat motor cortex for which it was determined based on the results of an analysis of activity fluctuation in the resting animal (Efron and Tibshirani 1993; Stout and Beloozerova 2013). The portion of the step cycle, in which the discharge rate exceeded the value of the minimal rate plus 25% of the difference between the maximal and minimal rates in the histogram, was defined as a "period of elevated firing" (PEF; Fig. 5C and E). PEFs were smoothed by removing all 1-bin peaks and troughs. For neurons with a single PEF per step cycle, the "preferred phase" (PrPh) of the activity was calculated using circular statistics (Batshelet 1981; Drew and Doucet 1991; Fisher 1993; Beloozerova et al. 2003).

The following parameters of the activity were calculated for each neuron: the mean discharge rate, dM, the number of PEFs, the duration of PEF(s), and, for neurons with a single PEF per step cycle, the PrPh. For each neuron, the difference in each activity parameter between locomotion on the flat surface and the ladder was determined. For the comparison of the discharge frequency during different tasks, the Student's 2-tailed t test was used. When comparing dMs, PrPhs, and durations of PEFs, differences ≥2%, 10%, and 20%, respectively, were considered to be significant. These criteria were adopted to be the same as for the activity of neurons in the cat motor cortex for which they were determined based on the results of a bootstrapping analysis that compared differences in the activity parameters between various reshufflings of strides of the same locomotion task (Efron and Tibshirani 1993; Stout and Beloozerova 2013).

For populations of neurons, the following activity parameters were calculated and compared between locomotion tasks: the percentage of neurons at their PEF during different phases of the step cycle, the distribution of the average discharge frequency of the population over the step cycle, the range of coefficients of modulation, and the average width of PEFs. To evaluate whether neuronal samples were sufficiently large to characterize the activity of each subpopulation, from each sample, 4 subsets of 3/4 of the neurons were selected, and the profiles of the neuronal recruitment and average discharge rate were compared among these subsets. If reducing a subpopulation by a quarter did not significantly alter these profiles, the original sample was considered to be sufficiently large. The subsets were composed as follows: subset #1 lacked the first, fifth, ninth, 13th, etc. neurons from the original sequence; subset #2 lacked the second, sixth, 10th, 14th, etc. neurons; subsets #3 and #4 lacked the third, seventh, 11th, 15th, etc. neurons; and the fourth, eighth, 12th, 16th, etc. neurons, respectively. The difference of each parameter of population activity between tasks and groups of neurons was tested using Student's 2-tailed t test. Unless noted otherwise, for all mean values, the standard deviation (SD) is given. When data were categorical, a nonparametric Mann-Whitney (U) test or  $\chi^2$  test (Fisher's 2-tailed test) was performed. The level of significance for all tests was set at 0.05.

## Histological procedures

On the day of termination, cats were deeply anesthetized with pentobarbital sodium, and reference electrolytic lesions were made in the areas of recording and stimulation. Cats were perfused with 4% paraformaldehyde solution, and brains were harvested. Frozen brain sections, 40  $\mu$ m thick, were cut in the regions of recording and stimulation. The tissue was stained for the Nissl substance with cresyl violet or thionine. The positions of the recording tracks in area 5 were estimated in relation to the reference lesions. The positions of the stimulation electrodes in motor cortex, midbrain, and medullary pyramids were verified. Further details of histological procedures can be found in Favorov et al. (2015) and Marlinski, Nilaweera, et al. (2012).

## Results

## Area of recording

Recordings were obtained from the most rostral part of the suprasylvian gyrus. Figure 2A-D shows the entry points of microelectrode penetrations in which neurons were recorded in cat 1 (Fig. 2A and C; 27 penetrations) and cat 2 (Fig. 2B and D; 23 penetrations). Histological examination showed that all microelectrode tracks were made through the cytoarchitectonic area 5 (Hassler and Muhs-Clement 1964; Avendano et al. 1985, 1988). Figure 2E and F shows the rostral (E) and caudal (F) blocks of cat 1 brain, divided along line f in Fig. 2A and C. A photomicrograph of a parasagittal section through the rostral block in Fig. 2G features two reference lesions

discharged (arrow 1) and MCprox was stimulated 7 ms later (arrow 2). The CC did not respond (arrow 3) because in 7 ms its spontaneous spike was still en route to the site of stimulation in the MCprox, and thus collision/nullification of spontaneous and evoked spikes occurred. This confirmed the antidromic nature of the evoked spike. Five sweeps are superimposed. This CC was recorded in cat 1 from layers II-IV. In A), the entry point of the cortical track, from which this neuron was recorded, is highlighted with a white ring. C) Distribution of latencies of antidromic responses of all CCs. Values for all detected axonal branches are included, for a total of 256 branches originating from 226 CC neurons, with 24 neurons sending 2 or 3 branches to various sites. Vertical dashed line denotes the division (4 ms) between fast- and slow-conducting CCs. The mean latency and its SD for each group are stated. D) Distribution of the estimated conduction velocities of all detected axonal branches. Vertical dashed line denotes the division (3.8 m/s) between fast- and slow-conducting CCs (fCCs and sCCs). The mean velocity and its SD for each group are stated. E) Distribution of antidromic latencies of CCs located in cortical layers II–IV, all axonal branches. The dashed line denotes the division (4 ms) between fCCs and sCCs. F) Estimated axonal conduction velocities of CCs in cortical layers II-IV, all axonal branches. The dashed line denotes the division (3.8 m/s) between fCCs and sCCs. G, H) Distribution of antidromic latencies and estimated conduction velocities for CCs in cortical layer V. I, J) Same for CCs in layer VI.

between which a line of giant pyramidal cells in layer V characteristic for area 5 is visible; it is highlighted by a dashed line drawn below the layer. A photomicrograph of a frontal section through the caudal block in Fig. 2H shows a reference lesion in the lateral bank of the lateral sulcus, with a line of giant pyramidal cells in layer V seen across the crest of the suprasylvian gyrus and down the bank of the lateral sulcus; it is highlighted by a dashed line drawn below the layer. The border between areas 5a and 5b was not evaluated.

## Neuronal populations studied

The studied neuronal populations are detailed in Table 1. A total of 456 neurons were recorded: 191 in cat 1 and 265 in cat 2. Between 1 and 49 neurons were recorded in a penetration,  $7.1\pm4.0$  in cat 1 and  $11.5\pm11.8$  in cat 2. Of these, 227 (54 in cat 1 and 173 in cat 2) sent an axon to the ipsilateral motor cortex and thus were CCs. The entry points of microelectrode penetrations, from which CCs were collected in cat 1 (17 penetrations) and cat 2 (23 penetrations), are shown in Fig. 2A and B, respectively. Axons of 29 cells descended within the medullary pyramidal tract, identifying them as PTNs. In cat 1, 15 cells were identified as midbrain-projecting. Axonal projections of 185 neurons were not identified: 95 cells in cat 1 and 90 in cat 2. In this report, neurons with descending axons will be considered jointly with neurons whose axon projections were not identified. This combined group of 229 neurons (137 in cat 1 and 92 in cat 2) will be referred to as nonidentified cells (noIDs). The entry points of microelectrode penetrations, from which noIDs were recorded in cat 1 (27 penetrations) and cat 2 (18 penetrations), are shown in Fig. 2C and D, respectively. Although the activity of not identified neurons of area 5 in the cat during locomotion tasks identical to those used here was previously reported (Beloozerova and Sirota 2003), the group of noIDs included in this study is different in that it was collected from a smaller region of the cortex restricted to the forelimb-related area in the rostral part of the suprasylvian gyrus. In addition, this group was composed only of neurons recorded in the same or immediately adjacent microelectrode tracks to those, from which the CCs were recorded (Fig. 2A-D), with the specific purpose to serve as a reference group for these CCs.

Most CCs, 72% (163/227), were recorded in the upper cortical layers II-IV, 15% (35/227) were recorded in layer V, and 7% (17/227) in layer VI. Among noIDs, 25% (58/229) were in layers II-IV, 66% (152/229) in layer V, and 3 cells in layer VI. The layer position of 12 CCs and 16 noIDs was not identified.

## Axonal conduction times of CCs projecting to motor cortex

An example of the antidromic identification of a CC neuron is shown in Fig. 3B. This neuron consistently responded to electrical stimulation of MCprox (arrow 2) with a latency of 14.4 ms (arrow 3) but only when no

Table 1. Neuronal populations according to axonal projection

Axonal projection	Cat 1	Cat 2	Total
Corticocortical to	Rest/locom 54/30	Rest/locom 173/60	Rest/locom 227/90
motor cortex noID axon	137/137	92/92	229/229
Total	191/167	265/152	456/319
RF	Cat 1	Cat 2	Total
	noIDs/CCs	noIDs/CCs	noIDs/CCs
Head	3/1	6/4	9/5
Shoulder	28/6	4/2	32/8
Elbow	20/3	4/3	24/6
Wrist/paw	34/15	-/-	34/15
All forelimbs	10/1	-/1	10/2
Vision	7/-	32/16	39/16
No RF	4/3	25/61	29/64
Total	106/29	71/85	<b>177/114</b> (several cells are included in two RF groups)

spontaneous spikes occurred within this time prior to the stimulation (top vs. bottom trace; see figure legend for a detailed explanation).

The distribution of latencies of CC responses to electrical stimulation of motor cortex and the distribution of estimated axonal conduction velocities are shown in Fig. 3C-J. Axonal conduction times were typically short, with 70% of neurons responding with a latent period <6 ms (Fig. 3C). The estimated conduction velocities ranged between 0.4 and 18 m/s (Fig. 3D). We arbitrarily divided CCs into 2 groups: cells responding with a latent period of 4.0 ms or faster ("fast" CCs or fCCs, n = 117), and thus conducting with velocities of ~3.8 m/s or faster, and those responding with longer delays ("slow" CCs or sCCs, n = 110). In Fig. 3C-F, the fCCs and sCCs are separated with a vertical dashed line.

Out of 227 CCs tested, 24 had an axon branching to both MCdist and MCprox. Axonal conduction times and conduction velocities of axons to MCdist and MCprox were similar. In cat 1, 7 of 54 CC neurons sent an axon to area 6, and for 6 of them, it was in addition to an axon sent to MCprox (5 cells) or MCdist (1 cell). In each of the 24 neurons that had >2 axonal branches, all branches conducted either fast (12 neurons) or slowly (12 neurons). One CC had an axon branch that descended subcortically to the midbrain, and none had any branch descending within the pyramidal tract.

The axonal conduction times and conduction velocities of CCs differed by the cortical layer where the neuron's soma was located. In layers II-IV, they varied widely, like those of the whole CC population (Fig. 3E and F). By contrast, CCs of layer V consistently had short axonal conduction times and fast conduction velocities (Fig. 3G and H), while those in layer VI had long conduction times and slow velocities (Fig. 3I and J). The axonal conduction times of CCs in layer V were shorter and velocities were faster than those of fCCs in layers II-IV (P < 0.05, t test). Axonal conduction times and conduction velocities of CCs in layer VI were similar to those of sCCs in layers II-IV.

## Somatosensory and visual RFs of neurons

Somatosensory and visual RFs of 104 noIDs and 26 CCs in cat 1 and 65 noIDs and 83 CCs in cat 2 were tested (Table 1).

The majority of noIDs, 64% (109/169), responded to somatosensory stimulation. Example responses of two noIDs to flexion of the right shoulder are shown in Supplementary Fig. 1A. Nineteen percent (32/169) of noIDs responded to palpation of muscles on the upper back, neck, or chest (n=12), or to extension (n=12), flexion (n=6), or adduction/abduction (n=2) in the shoulder joint; they were jointly termed shoulder-related neurons. Fourteen percent (24/169) of noIDs responded to movement in the elbow joint (n = 18), including 7 that were activated by elbow extension and 6 by elbow flexion, or to palpation of arm muscles (n = 6); they were jointly named elbow-related neurons. Twenty percent (34/169) of noIDs responded to palpation of the paw (n=22), including 5 neurons with an RF on toes, to palpation of the forearm and wrist (n=4), or to ventral (n=7) or dorsal (n=1) flexion of the wrist; they were jointly termed wrist/paw-related neurons. In addition, 6% (10/169) of neurons responded to manipulation of any part of the right forelimb. Finally, 5% (9/169) of cells responded to touching of the head (the ear, forehead, cheek, whiskers, or chin) and were named head-related neurons. RFs of all but 3 cells were on the right side of the body, that is, contralateral to the left cortex recorded, and all but one were excitatory. Seven of 9 neurons with a somatosensory RF on the head also responded to visual stimulation (see below). Neurons with RFs on different segments of the body were distributed across the cortical layers similarly to the entire sample except that shoulder-related cells were more often found in layer V (P = 0.007,  $\chi^2$  test).

Only about 1/3 of CCs (33/109) responded to somatosensory stimulation, a much smaller proportion compared to noIDs (P < 0.001,  $\chi^2$  test). RFs of all but one CC were located on the contralateral (right) side of the body: 5 cells were activated by a touch to the head (the ear, forehead, cheek, whiskers, or chin); 8 were activated by movement in the shoulder joint or palpation of the upper back muscles; 6 cells were activated by a movement in the elbow joint, including 3 that also responded to manipulation of the shoulder; 15 CCs were activated by palpation of the forearm, paw, or by dorsal flexion of the wrist; and RFs of 2 cells covered the entire forelimb. Most somatosensory responsive CCs (22/109) were in cortical layers II-IV and the majority were fast-conducting (27/109). The proportions of CCs that responded to somatosensory stimulation in layers II–IV and layer V were similar.

About 1/4 of noIDs (39/169) responded to visual stimulation. Example responses of 2 noIDs to an approaching object (a cat toy) are shown in Supplementary Fig. 1B. Responses of 14% (24/169) of neurons were directionspecific: 12 cells were activated by a stimulus moving downward, whereas only 1 cell preferred the upward movement; 6 neurons were activated by an approaching stimulus, and 4 were activated by a stimulus moving from the ipsi- to contralateral side of the visual field, whereas only 1 preferred the opposite direction. Among neurons responsive to visual stimulation, 8 also responded to somatosensory stimulation of the face (n=7) or forelimb (n=1). The majority of visually responsive noIDs (25/169) were in cortical layer V.

The proportion of visually responsive cells among CCs was similar to that among noIDs, 15% (16/109). Of these, 7 were activated by a stimulus moving downward, 2 responded to both the downward and upward movements, 4 were activated by a stimulus moving from the ipsi- to contralateral side of the visual field, and 3 had a less defined field. Four of the visually responsive CCs were also activated by somatosensory stimulation of the head or movement in the shoulder joint. Half of visually responsive CCs (n=9) were in cortical layers II-IV and all but one were fast-conducting. The proportions of visually responsive cells in layers II-IV and layer V were

Only 17% (29/169) of noIDs did not have a somatosensory or visual RF that we could detect in the sitting cat. Half of these (n = 14) were located in cortical layers II–IV, 11 were in layer V, and 2 were in layer VI. In sharp contrast, most CCs, 59% (64/109), did not have a somatosensory or visual RF, a much larger proportion than among noIDs (P < 0.001,  $\chi^2$  test). Most of these CCs (n = 39) were in cortical layers II–IV and the majority were slow-conducting (n = 39, not same cells). In fact, CCs that did not have a somatosensory or visual RF had axons that conducted substantially slower than axons of CCs that had an RF (6.4  $\pm$  5.3 vs. 2.4  $\pm$  2.0 ms for latent periods of antidromic responses and  $4.6 \pm 4.0$  vs.  $7.7 \pm 4.0$  m/s for conduction velocity; P < 0.0001 for both, t test).

### Activity of neurons in the sitting or standing cat

The overwhelming majority of noIDs, 74% (102/137) in cat 1 and 91% (84/92) in cat 2 (186/229 total), were active when the cat was sitting or standing. The proportion of active cells was greater in layers II–IV where 93% (54/58) were active than in layer V, where only 77% (117/152) were active (P = 0.007,  $\chi^2$  test). However, the discharge rate of active noIDs in layer V was more than double of that of active noIDs in layers II–IV:  $10.9 \pm 8.9$  vs.  $4.1 \pm 6.2$ spikes/s (P < 0.001, t test; Fig. 4A, light gray bars). The average discharge rate of the entire noID population was  $6.9 \pm 8.5$  spikes/s.

From 112 CCs tested, 73% (22/30) in cat 1 and 48% (39/82) in cat 2 (61/112 total) were active when the cat was sitting or standing. For cat 1, this proportion was similar to that of noIDs, whereas for cat 2 it was smaller.

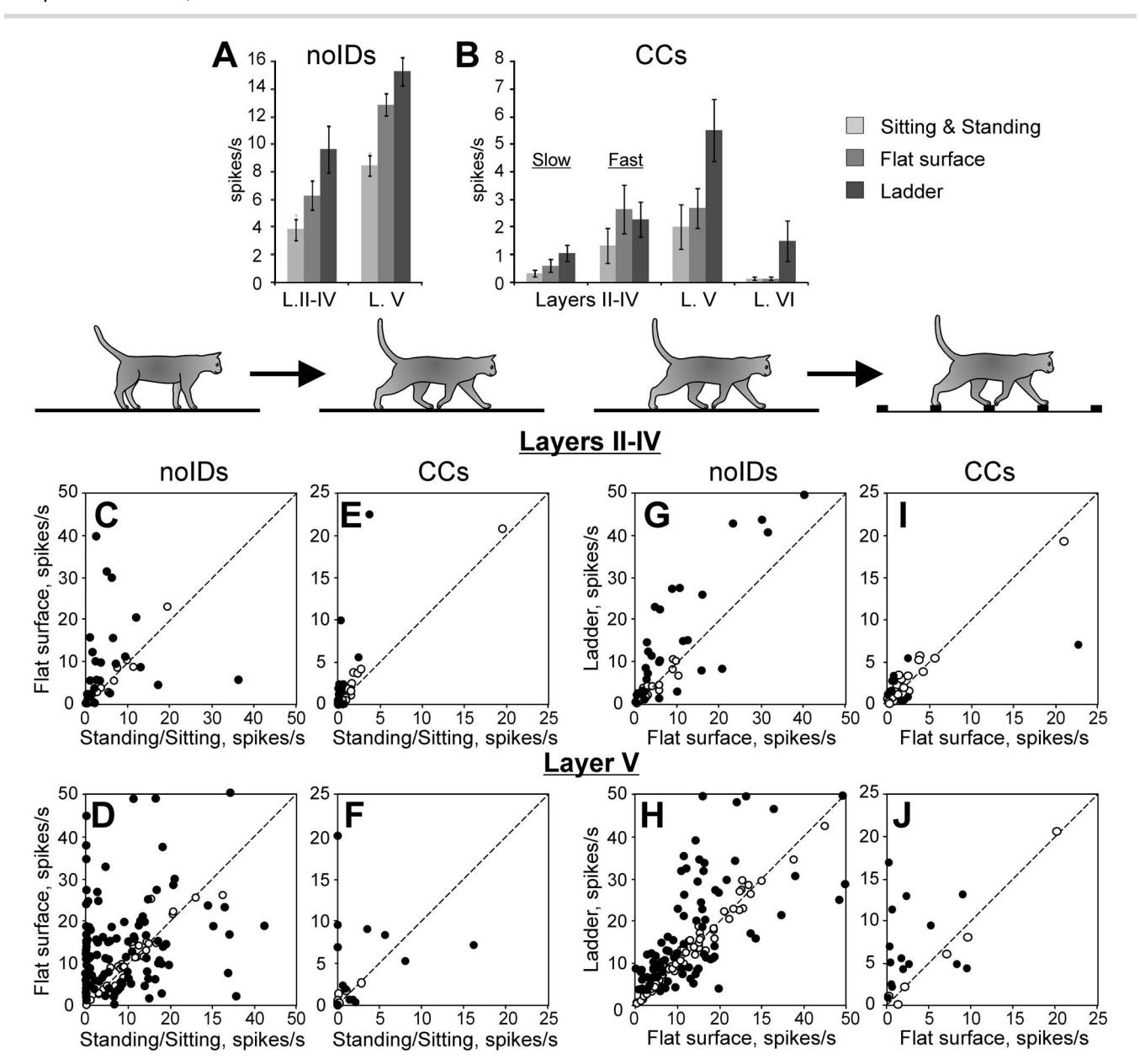


Fig. 4. Discharge rates of subpopulations of neurons during different tasks. A, B) Average activity of neurons in different cortical layers (includes both active and inactive cells). L.II–IV, layer II–IV; L.V, layer V; L.VI, layer VI. For layers II–IV, the averages for slow- and fast-conducting CCs are plotted separately. Note that in A and B the ordinate scales are different. Error bars show SEM. C–F) Comparison of the discharge rate of individual noID (C, D) and CC (E, F) neurons during sitting or standing and locomotion on the flat surface. The x- and y-axes of each point show the discharge rate of a neuron during sitting or standing and locomotion, respectively. Neurons whose discharge rates were statistically significantly different between the tasks are shown by filled symbols, the others are shown by open symbols. G–J) Comparisons of the discharge rate of individual noID (G, H) and CC (I, J) neurons during locomotion on the flat surface and the ladder. C, E and G, I) Cells located in layers II–IV. D, F and H, J) Cells located in layer V. Note that the scales for CCs activity plots E, F and I, J are twice as large as those for noIDs plots C, D and G, H.

The discharge rate of the entire CCs population was  $1.6\pm4.3$  spikes/s, only a quarter of that of noIDs. As in the noID population, the recruitment and discharge rate of CCs differed by cortical layer but differently from noIDs. In layers II–IV, only 47% (35/75) of CCs were active, which was a much smaller proportion than among noIDs (P < 0.001,  $\chi^2$  test). Although the recruitment of fCCs at 57% tended to be larger than that of sCCs, and fCCs were more active, the whole group of layers' II–IV CCs discharged with much lower rates than noIDs, producing only  $1.4\pm5.9$  spikes/s (P < 0.04, t test; Fig. 4A and B, light gray bars). In layer V, 59% (13/22) of CCs were active,

which was similar to noIDs in this layer. These CCs discharged  $3.4\pm4.5$  spikes/s, which was a similar rate to that of the fast-conducting CCs in layers II–IV and tended to be higher than the rate of the slow-conducting CCs in these layers. However, this was less than half of the discharge rate of the active noIDs in layer V (P < 0.001, t test; Fig. 4A and B, light gray bars). In layer VI, only 1/3 (6/18) of CCs was active and their discharge at  $0.4\pm0.2$  spikes/s was lower than that of CCs in layer V (P=0.03, t test; Fig. 4B).

Thus, when the cat was sitting or standing, only half of area 5 CCs in layers II–IV were conveying any information

to motor cortex. Their signal was 4 times weaker than that of the neighboring noIDs. The fCCs tended to be slightly more engaged and active than sCCs. In layer V, the recruitment of CCs was similar to that of noIDs, however, their discharge rate was less than half of that of noIDs.

#### Characteristics of locomotion

During recording of each neuron, cats walked between 7 and 47 times down each corridor (25  $\pm$  8). The number of strides selected for the analysis according to the criteria described in the Methods was  $56 \pm 21$  for the flat surface and  $39 \pm 14$  for the ladder. For different neurons, the average duration of the strides varied between 510 and 870 ms, which corresponded to the speed of 0.6–1.0 m/s. Cat 1 walked slightly slower than cat 2 with  $738 \pm 63$  ms long strides both on the flat surface and the ladder (Fig. 1B). The strides of cat 2 on the flat surface were  $645 \pm 48$  ms, and they were slightly shorter on the ladder,  $622 \pm 60$  ms (Fig. 1B). In both cats, the proportion of the stance phase in the step cycle (the stride duty factor) was smaller during the ladder task, however, the difference was small, 2-5% (Fig. 1C).

## Activity during locomotion on the flat surface

As explained above, many studies showed that locomotion on the flat surface does not require vision and can be accomplished without the forebrain. We will first describe the activity of the diverse group of noIDs and then compare the activity of the neighboring CCs projecting to motor cortex to the activity of noIDs to understand how well CCs reflect the activity of the broad area 5 population during this cortex-independent and vision nonrequiring task and whether they transmit any signals of their own.

## noIDs

Example activity of a noID neuron during locomotion is shown in Fig. 5A-E. When the cat was standing, the neuron discharged ~3 spikes/s. During locomotion on the flat surface, the discharge frequency was much higher, ~25 spikes/s, and was weakly modulated with the rhythm of strides (Fig. 5A, left side; Fig. 5B). The activity is summed in Fig. 5C that shows the distribution of the discharge frequency across the step cycle. The discharge was greater during late swing and stance and smaller during first half of swing, and the dM was 5.3.

All noIDs recorded in the sitting or standing cat were also recorded as the cat walked on the flat surface: 137 in cat 1 and 92 in cat 2 (229 in total, Table 1). Unlike during sitting or standing, when 9-26% of noIDs were silent, when the cat walked, 99% were active (227/229). The average discharge was  $10.9 \pm 10.0$  spikes/s, higher than during sitting or standing, even when only cells that were active in those conditions were considered (P = 0.01, t test). The increase in the activity was caused by an increase in 56% (129/229) of cells by  $9.8 \pm 9.4$  spikes/s on average, while the activity of only 20% (46/229) decreased. Layer V noIDs

that increased activity increased it more than noIDs in layers II–IV by  $11.1 \pm 9.5$  vs.  $6.0 \pm 8.6$  spikes/s (P = 0.007, t test; Fig. 4C and D). As at rest, noIDs in layer V were twice more active than in layers II–IV, discharging  $12.7 \pm 10.3$ spikes/s vs.  $6.3 \pm 8.3$  spikes/s (P < 0.001, t test; Fig. 4A, medium gray bars). The discharge rate of all but 2 noIDs was high enough to generate a step phase distribution histogram, and the activity of 87% (197/227) of them was modulated with the rhythm of strides, i.e. like the activity of the example neuron shown in Fig. 5A–E, it was greater in one phase of the stride and smaller in another phase. Two basic patterns of modulation were observed: with one period of elevated firing, 1-PEF, or two periods, 2-PEF (see Methods for the PEF definition).

The 1-PEF pattern was more common, expressed by 64% (146/227) of cells, while 21% (48/227) had 2 PEFs. In addition, 3 noIDs had 3 PEFs, and they will be considered jointly with the 2-PEF group. The average duration of PEFs in the 1-PEF group was  $59\% \pm 20\%$  of the cycle, and the combined duration of PEFs in the 2-PEF group was similar, 57% ± 14%. In both subpopulations, PEFs of different neurons were distributed over the step cycle and overlapped (Fig. 6A1 and B1). In the 1-PEF group, the neurons with PEFs in the beginning of swing and end of stance were more active, causing the activity of the population to peak in early swing (Fig. 6A2 and A4). The 2-PEF noIDs were only half as active as the 1-PEFs, firing  $6.4 \pm 5.5$ spikes/s vs.  $11.7 \pm 10.5$  spikes/s (P < 0.001, t test; Fig. 6B2 and B4 vs. Fig. 6A2 and A4). The beginnings of the two PEFs were separated by  $\sim$ 50% of the cycle (46%  $\pm$  14%). The 2-PEF group activity had a prominent peak at the end of stance and a subtle one during transition from swing to stance. Discharges of individual 1-PEF and 2-PEF noIDs were modulated with a similar average magnitude (dM:  $10.9 \pm 6.9$  and  $9.7 \pm 4.9$ , respectively).

Cortical layers II–IV and V were slightly different in the proportion of 1-PEF and 2-PEF noIDs. The proportion of 1-PEFs in layers II-IV was smaller than in layer V  $(53\% [31/58] \text{ vs. } 68\% [103/152]; P = 0.05, \chi^2 \text{ test}), \text{ while}$ the proportion of 2-PEFs tended to be larger (31% [18/58] vs.19% [29/152]; P = 0.06,  $\chi^2$  test). The group activity of 1-PEF noIDs in layers II–IV was fairly constant over the cycle at  $7.2 \pm 8.5$  spikes/s (Fig. 7A2 and A4), while in layer V, it was stride phase-modulated peaking during swing and was higher overall  $(13.3 \pm 10.8 \text{ spikes/s}; P = 0.002, t \text{ test};$ Fig. 7C2 and C4). The activity of 2-PEF noIDs in layers II-IV was very low,  $2.2 \pm 2.0$  spikes/s, and barely modulated (Fig. 7B2 and B4). By contrast, the activity of the 2-PEF group in layer V was modulated with a major peak at the end of stance (Fig. 7D2 and D4). Across the 1-PEF and 2-PEF groups, the activity of individual noIDs in layers II–IV was more stride phase-modulated than in layer V, with the dM of  $12.5 \pm 7.8$  vs.  $9.3 \pm 5.2$  (P < 0.02, t test).

#### CCs

Example firing behavior of a low-active CC neuron (cell #1469) during locomotion is shown in Fig. 5F-J. When the cat was sitting or standing, or walked on the flat

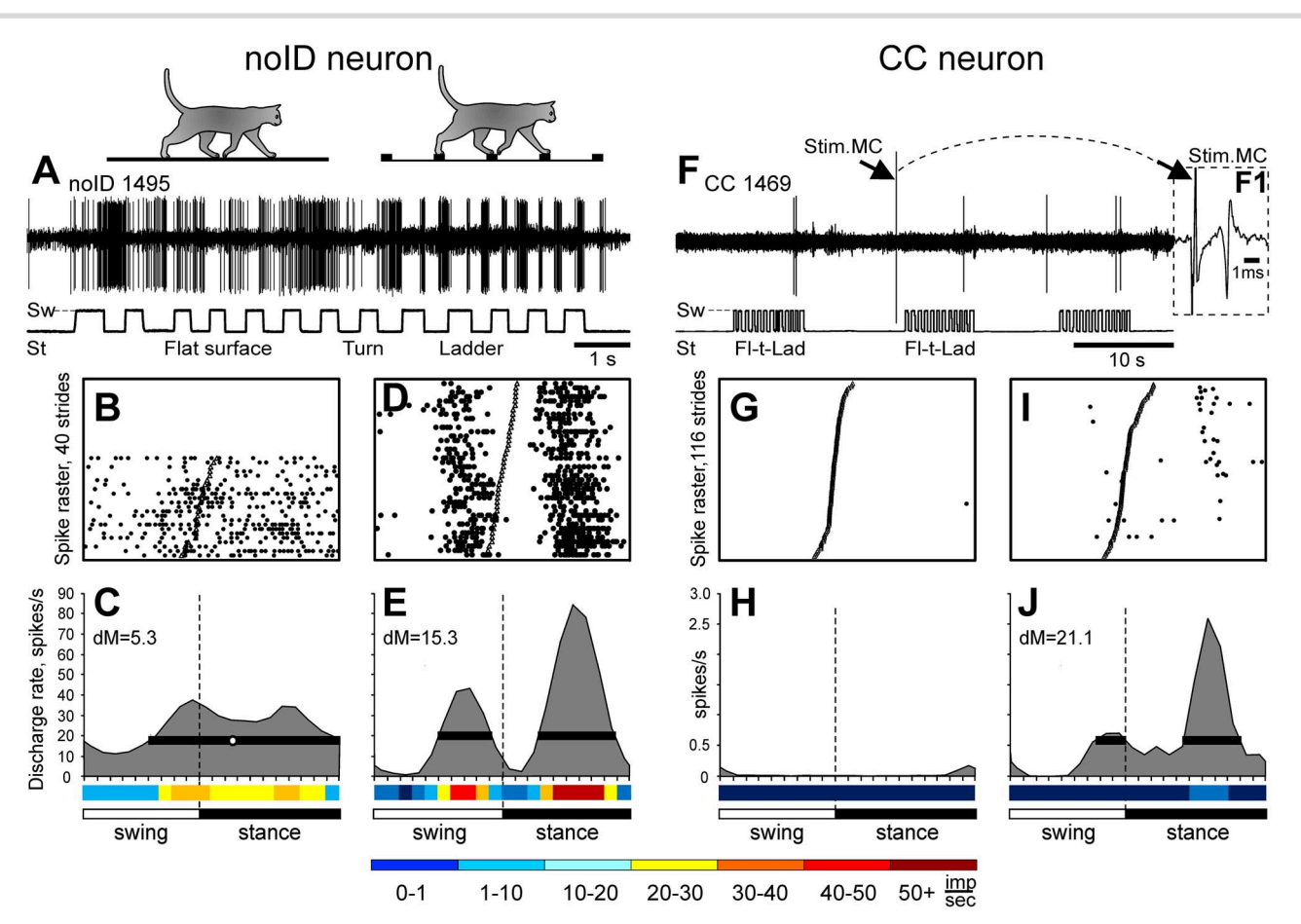


Fig. 5. Example activity of a noID and a CC neurons during locomotion on the flat surface and the horizontally placed ladder. A-E) Activity of a noID neuron (cell #1495) during locomotion. The neuron recorded in cat 2 was located medially in the rostral suprasylvian gyrus and was situated in cortical layer V. In Fig. 2D, the track where it was encountered is highlighted with a white ring. A) Discharges of the noID during 1 round of locomotion. Silhouettes of cats at top indicate locomotion on the flat surface (left) and the ladder (right). Bottom trace shows the swing (deflection up) and stance (deflection down) phases of the step cycle of the right forelimb. B, C) Activity of the same noID neuron during locomotion on the flat surface is presented as a raster of 23 step cycles B) and a histogram C). In the raster, the duration of step cycles is normalized to 100%, and the cycles are rank-ordered according to the duration of the swing phase. The beginning of the stance phase in each step cycle is indicated by an open triangle. In the histogram, the horizontal black bar shows the PEF, and the circle indicates the PrPh. The value of the depth of the activity modulation (dM) is indicated. The rainbow bar below the histogram shows the average discharge frequency of the neuron in each 1/20th portion of the step cycle, color-coded according to the scale at bottom of the figure. Periods of the swing and stance phases of the stride of the right forelimb are indicated by white and black horizontal bars, respectively. D, E) Activity of the same noID neuron during locomotion on the ladder. F-J) Activity of a CC neuron (call #1469) during standing and locomotion. This neuron also recorded in cat 2 was located medially in the rostral suprasylvian gyrus, just ~1 mm away from noID #1495, the activity of which is illustrated in A-E). The track where it was encountered is highlighted in Fig. 2B with a white ring. This CC neuron was situated in layers II-IV and responded to electrical stimulation of MCdist with the latency of 2.1 ms, thus was a fCC (Stim.MC in F, insert F1). F) Discharges of the CC neuron during 3 rounds of locomotion in the chamber. The cat started each round by walking on the flat surface (Fl), then turning (t) onto the ladder (Lad). Bottom trace shows swing and stance phases of the right forelimb. During ~50 s shown in the figure, the CC discharged 6 spikes, all but 1, while the cat was on the ladder. A stimulus was applied to motor cortex shortly before the second round. The response of the cell is shown at a fast time scale in insert F1. G, H) Activity of the same CC neuron during locomotion on the flat surface is shown as a raster of 116 step cycles (G) and a histogram (H). The CC discharged only 1 spike during 116 strides. I, J) Activity of the same CC neuron during locomotion on the ladder shown as a raster (I) and a histogram (J).

surface, the neuron was essentially silent, discharging only a handful of spikes at rest and only 1 spike during 116 strides on the flat surface (Fig. 5F, G, H).

The activity of 90 CCs was tested while the cat walked on the flat surface: 30 in cat 1 and 60 in cat 2 (Table 1). This was a subset of 112 CCs, the activity of which was recorded when the cat was sitting or standing. Unlike in those conditions, when half of CCs were silent, when the cat walked, 97% of CCs (29/30) in cat 1 and 73% (44/60) in cat 2 were active (73/90 neurons total). The discharge rate increased in 34% (31/90) of cells, by  $3.5 \pm 5.2$  spikes/s on average, while decreasing in only 12% (Fig. 4E and F). However, compared to noIDs, the proportion of CCs increasing activity with the start of locomotion was substantially smaller (P < 0.001,  $\chi^2$  test), and the increase

was smaller (P < 0.001, t test; Fig. 4C–F). In result, as during sitting or standing, the average discharge rate of CCs during locomotion on the flat surface was only  $\sim 1/5$ th of that of noIDs.

Activity averages by cortical layer are shown in Fig. 4B (medium gray bars). The active fCCs in layers II–IV producing  $3.0\pm5.4$  spikes/s were now as active as CCs in layer V and were substantially more active than the active sCCs in layers II–IV, which produced only  $0.9\pm1.1$  spikes/s (P=0.05, t test). The discharge rate of CCs in layer VI was as low as that of sCCs in the upper layers (0.2  $\pm$  0.2 spikes/s). Unlike layer V noIDs that increased activity with the start of locomotion more than their peers in layers II–IV (Fig. 4A), the activity increase of layer V CCs was similar to that of fCCs in layers II–IV

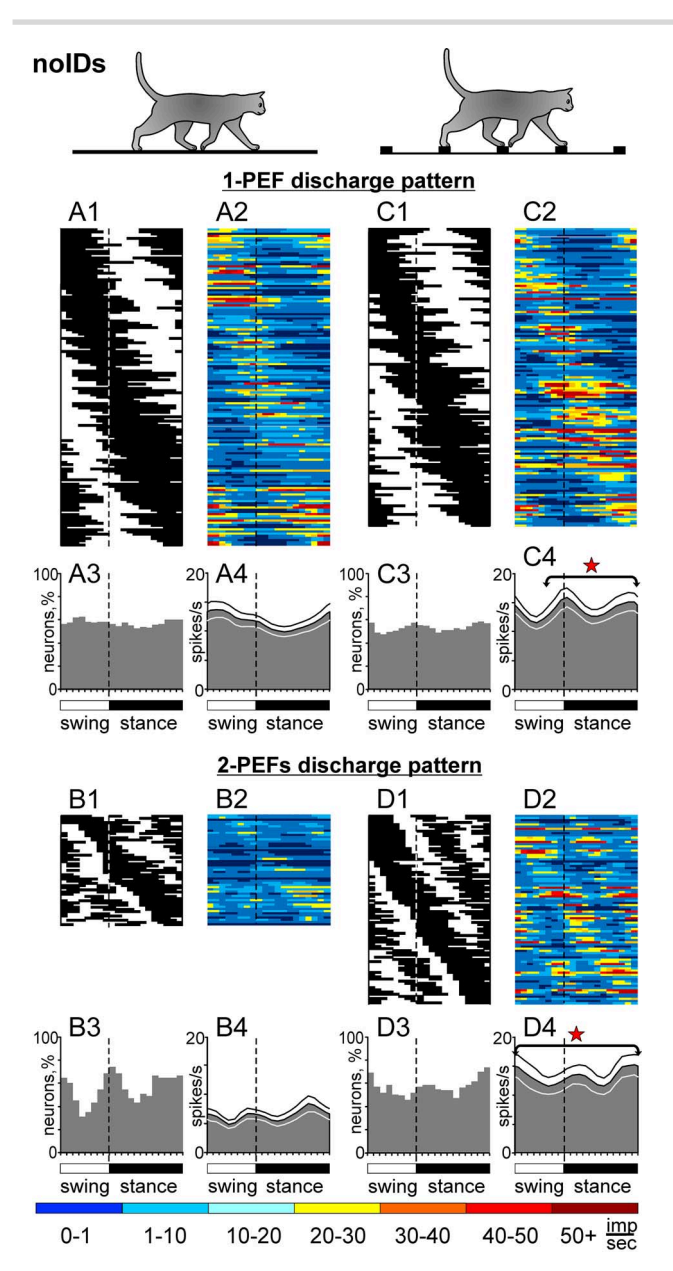


Fig. 6. Population characteristics of noID neurons with 1-PEF and 2-PEF discharge patterns. Activity of neurons discharging with a 1-PEF (A, C) or 2-PEF (B, D) pattern during locomotion on the flat surface (A, B) and the ladder (C, D). A1, B1, C1, D1) Phase distributions of PEFs. Each horizontal bar represents the PEF location of 1 neuron relative to the step cycle. Neurons are rank ordered so that those active earlier in the cycle are plotted at top of the graph. A2, B2, C2, D2) Corresponding phase distributions of discharge frequencies. Average discharge frequency in each 1/20th portion of the cycle is color-coded according to the scale shown at bottom of the figure. A3, B3, C3, D3) Proportion of active neurons (neurons in their PEF) in different phases of the step cycle during flat surface (A3, C3) and ladder (B3, D3) locomotion. A4, B4, C4, D4) The mean discharge rate during the stride of flat surface (A4, C4) and ladder (B4, D4) locomotion. Thin lines show SEM. Red stars indicate periods of the stride when the activity during ladder locomotion was significantly greater than during flat surface locomotion (P < 0.05, U test). In each panel, a vertical interrupted line denotes the average end of the swing and beginning of the stance phase of the right forelimb.

(Fig. 4B). Because a number of CCs in layer V decreased activity, their population discharge did not change with the start of locomotion. The average firing rates of sCCs in layer II–IV and CCs in layer VI also did not change when locomotion began (Fig. 4B).

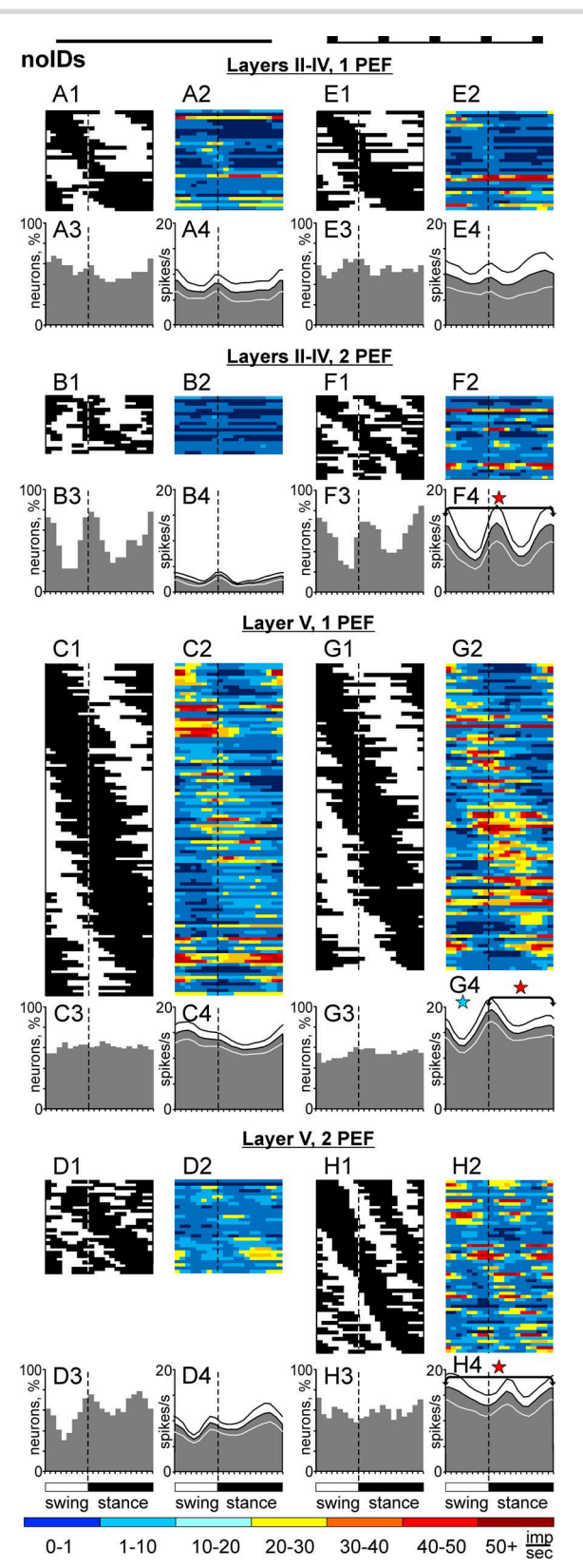


Fig. 7. Population characteristics of 1-PEF and 2-PEF noID neurons, subdivided by cortical layer position of their somata. Activity of neurons discharging with a 1-PEF (A, C, E, G) or 2-PEF (B, D, F, H) pattern during locomotion on the flat surface (A, B, C, D) and the ladder (E, F, G, H). A, E) Layers II–IV neurons discharging with a 1-PEF pattern during flat surface (A) and ladder (E) locomotion. B, F) Layers II–IV neurons discharging with a 2-PEF pattern. C, G) Layer V neurons with a 1-PEF discharge pattern. D, H) Layer V neurons with a 2-PEF discharge pattern. The blue star indicates the period of the stride when the activity during ladder locomotion was significantly smaller than during flat surface locomotion (P < 0.05, U test). Other designations are as described in Fig. 6.

Out of 73 CCs that were active during locomotion on the flat surface, only 59 discharged >1 spike during this task. The discharge of all but 2 of these cells was stride phase-modulated. They constituted 63% (57/90) of the entire CC population, a much smaller proportion than among noIDs (P < 0.001,  $\chi^2$  test). However, the dM was  $15.7 \pm 7.6$  on average, which was substantially greater than in the noID group (P < 0.001, t test). As among noIDs, two basic patterns of modulation were observed: with 1 or 2 PEFs. The 1-PEF pattern was also more common, expressed by 68% (39/57) of CCs, while 26% had 2 PEFs, and 5% had 3. CC and noID populations with stride-related activity were similar in the proportions of neurons with 1-, 2-, and 3-PEF discharge patterns  $(P > 0.05, \chi^2 \text{ test})$ . The average duration of PEFs in the 1-PEF CC group was 49% ± 21% of the step cycle,  $\sim$ 10% smaller than that of noIDs (P=0.01, t test). The combined duration of PEFs in the 2-PEF group was similar,  $51\% \pm 14\%$ . As in the noID population, PEFs of different CCs were distributed over the step cycle and overlapped (Fig. 8A1 and B1). The activity of the 1-PEF group was fairly steady across the cycle at ~4 spikes/s (Fig. 8A2 and A4). This was different from the activity of 1-PEF noIDs that had a peak during swing (Fig. 6A2 and A4). Like 2-PEF noIDs, 2-PEF CCs were much less active than their 1-PEF counterparts, discharging  $1.0 \pm 0.9$  vs.  $3.8 \pm 5.1$  spikes/s (P = 0.002, t test; Fig. 8B2 and B4 vs. A2 and A4). Also similar to noIDs, the beginnings of the two PEFs in 2-PEF CCs were separated by ~50% of the cycle  $(43\% \pm 15\%)$ . The activity of individual 1-PEF and 2-PEF CCs was modulated similarly, with the dMs  $16.3 \pm 8.7$  and  $14.4 \pm 4.4$ , respectively.

The 1-PEF and 2-PEF CCs were evenly distributed across cortical layers. In layers II-IV, the activity of 1-PEF CCs fluctuated over the step cycle peaking in the beginning of swing and end of stance (Fig. 9A2 and A4). This was different from the group activity of 1-PEF noIDs in layers II-IV, which was steady over the cycle (Fig. 7A2 and A4). The discharge rate of 2-PEF CCs in layers II-IV was very low, 1-2 spikes/s, and, similarly to that of 2-PEF noIDs, did not change over the cycle (Figs. 9B2 and B4 and 7B2 and B4). In layer V, the activity of 1-PEF CCs was fairly steady at ~5 spikes/s (Fig. 9C2 and C4), which differed from the modulated activity of layer V 1-PEF noIDs (Fig. 7C2 and C4). The discharge rate of 2-PEF CCs in layer V was low, 1-2 spikes/s, and did not change over the cycle (Fig. 9D2 and D4). This too was different from the modulated activity of 2-PEF noIDs in layer V that peaked in late stance (Fig. 7D2 and D4). Across the 1-PEF and 2-PEF CC groups, the average dM of individual cells in layers II-IV and V was similar, ~15, which was higher than the dM of noIDs in either layer (P < 0.04,

Thus, area 5 CCs as a group sent only a soft signal to motor cortex that the subject is now walking rather than sitting or standing. During locomotion on the flat surface, the activity of CCs was very low. Discharges of most individual cells were step cycle-modulated showing

the same two patterns as noIDs, and the dM was higher than in noIDs. However, the activity profiles of 1-PEF and 2-PEF CC subpopulations did not match those of noIDs, particularly in layer V. During this vision nonrequiring locomotion task, these CCs, as groups, transmitted their own signals to motor cortex, which were very low-rate and steady over the step cycle.

## Activity during vision-guided stepping on the horizontal ladder

Many studies have demonstrated that accurate stepping on a complex surface, such as the horizontal ladder, relies on vision and participation of the cortex (Trendelenburg 1911; Liddell and Phillips 1944; Chambers and Liu 1957; Beloozerova and Sirota 1988, 1993a, 2003; Metz and Whishaw 2002; Farr et al. 2006; Friel et al. 2007). To determine which part of the activity of CC and noID neurons during locomotion on the ladder is related to the processing of visual information as opposed to the movement itself, we compared the activity of the same neurons during vision-guided locomotion on the ladder with that during vision-independent locomotion on the flat surface. Since we have shown earlier that the biomechanics of locomotion on the convenient ladder used in this study are very close to those on the flat surface (Beloozerova et al. 2010), we reasoned that any difference will be primarily related to the processing of visual information for accurate stepping on the ladder. To understand which part of the vision processing-related information obtained by the broad area 5 population is conveyed by CCs to motor cortex and what signals, if any, CCs are relaying on their own accord, we compared the activity of CCs with that of noIDs.

## noIDs

Example activity of a noID neuron during locomotion on the flat surface and the ladder is shown in Fig. 5A-E. During ladder locomotion, the average discharge of the neuron was similar to that on the flat surface, ~27 spikes/s, however, the activity was much more modulated. The dM was 15.3 rather than 5.3. In addition, instead of discharging one long PEF, the neuron discharged two shorter PEFs.

The same 229 noID neurons, that were tested on the flat surface, were tested on the ladder (Table 1). All but 1 were active. The average discharge was  $13.5 \pm 12.6$ spikes/s, which was slightly higher than on the flat surface and twice as high than during sitting or standing (P = 0.004 and P < 0.001, respectively, t test). The increased population activity upon the flat surface-to-ladder transition was due to an activity increase of 41% (94/229) of neurons, by  $8.8 \pm 8.2$  spikes/s, while the activity of only 14% (33/229) decreased. The proportions of cells increasing and decreasing activity were similar between cortical layers II-IV and V (Fig. 4G and H). This caused the activity in layer V to remain higher than in layers II-IV,  $15.0 \pm 12.5$  vs.  $9.6 \pm 13.0$  spikes/s (P = 0.01, t test; Fig. 4A, dark gray bars).

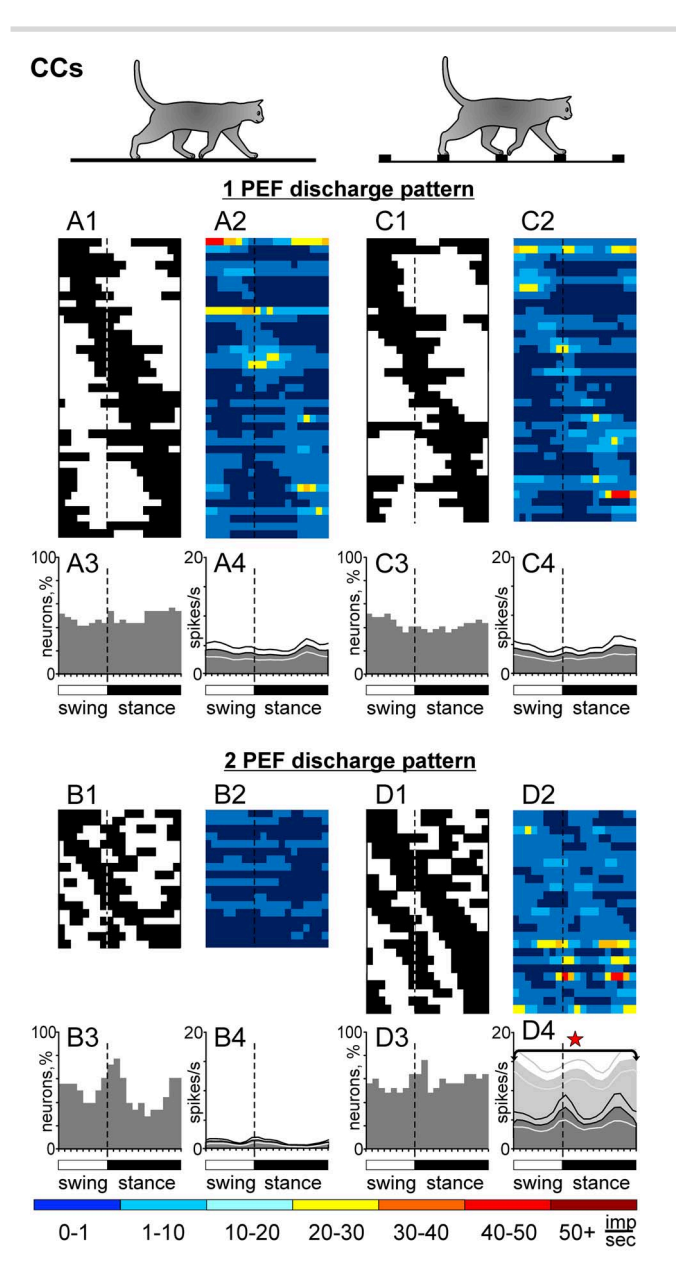


Fig. 8. Population characteristics of CC neurons projecting to motor cortex that discharge with a 1-PEF or 2-PEF pattern. Activity of neurons discharging with a 1-PEF (A, C) or 2-PEF (B, D) pattern during flat surface (A, B) and ladder (C, D) locomotion. In D4, the activity profile of noIDs from Fig. 6D4 is replotted as a light gray area graph in the background to facilitate comparison with the activity profile of CCs. Designations are as described in Fig. 6.

The discharge rate of all but 1 cell was high enough to generate a step phase distribution histogram, and the activity of 98% (224/228) of these neurons was modulated with the rhythm of strides. This was a larger proportion than on the flat surface (P < 0.001;  $\chi^2$  test). The dM was  $11.7 \pm 5.7$  on average, which was similar to that on the flat surface. The same two basic patterns of modulation were observed: with 1 or 2 PEFs. As on the flat surface, the 1-PEF pattern was more common, displayed by 60% (137/228) of neurons, while 38% (86/228) had 2 PEFs, and 1 cell had 3 PEFs. The proportion of 1-PEF cells was similar to that on the flat surface, while the proportion of 2-PEF cells was almost twice as large (P < 0.001,  $\chi^2$  test,

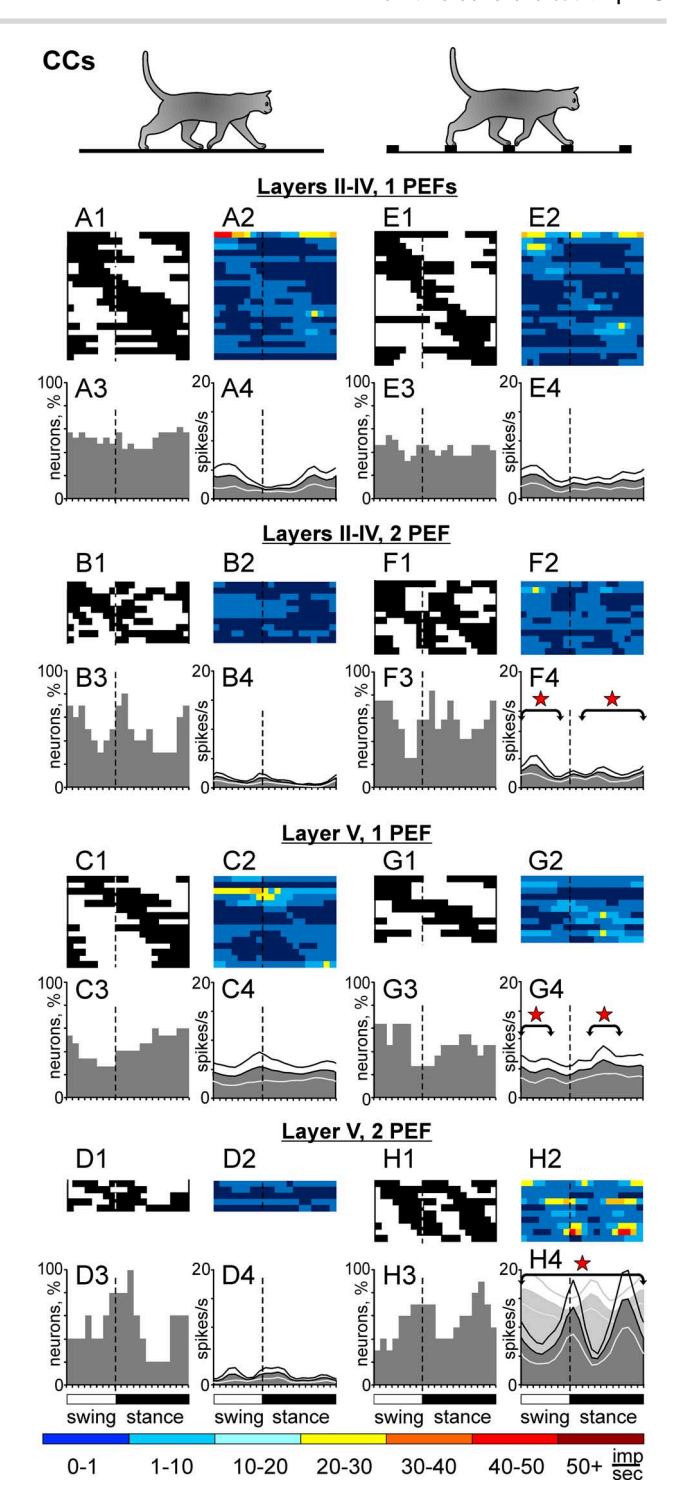


Fig. 9. Population characteristics of 1-PEF and 2-PEF CC neurons projecting to motor cortex, subdivided by cortical layer position of their somata. Activity of neurons discharging with a 1-PEF (A, C, E, G) or 2-PEF (B, D, F, H) pattern during locomotion on the flat surface (A, B, C, D) and the ladder (E, F, G, H). In H4, the activity profile of noIDs from Fig. 7H4 is replotted as a light gray area graph in the background. Designations are as described

Fig. 6C1 and D1 vs. A1 and B1). This was because half of noIDs, the activity of which was not stride-modulated on the flat surface (56%,18/32), had 2 PEFs on the ladder. In addition, 29% (42/146) of the cells that had 1 PEF on the flat surface had 2 PEFs on the ladder. The average duration of PEFs in the 1-PEF group and the combined

duration of PEFs in the 2-PEF group were similar,  $55\% \pm 18\%$  of the cycle, which was similar to their duration on the flat surface.

As on the flat surface, PEFs of neurons in both the 1-PEF and 2-PEF groups were distributed over the step cycle (Fig. 6C1 and D1). In the 1-PEF group, the average discharge at  $13.7 \pm 12.9$  spikes/s was similar to that on the flat surface. However, neurons with PEFs during the swing-to-stance and stance-to-swing transitions were more active than others and caused the 1-PEF population activity to have two subtle but statistically significant peaks during these transition phases (P=0.008, U test; Fig. 6C2 and C4). This was different from this group activity on the flat surface where it had a single peak in early swing (Fig. 6A2 and A4). Unlike 1-PEF noIDs, 2-PEF cells were twice more active on the ladder than on the flat surface, discharging  $13.1 \pm 12.1$  spikes/s (P < 0.001, t test; Fig. 6B4 and D4) and were now as active as 1-PEF noIDs. The discharge of the 2-PEF population too had two subtle peaks around the same phases of the stride (P = 0.01, U test; Fig. 6D4). The activity of individual 2-PEF noIDs was less modulated than that of individual 1-PEF cells, the dM averaged  $10.6 \pm 4.7$  vs.  $12.4 \pm 6.2$  (P = 0.02, t test).

Cortical layers II-IV and V did not differ in the proportions of 1-PEF and 2-PEF noIDs as they did during locomotion on the flat surface. This was because upon transition to the ladder, the proportion of 1-PEF cells in layer V decreased while that of 2-PEFs increased, which made them both similar to those in layers II–IV where the proportions did not change. In layers II–IV, the activity of the 1-PEF population was evenly distributed over the cycle, as on the flat surface, and was similar on average,  $9.0 \pm 13.8$  spikes/s (Fig. 7E2 and E4). By contrast, the activity of 2-PEF cells was sharply modulated with 2 peaks during stance-to-swing and swing-to-stance transitions (Fig. 7F2 and F4). Their average discharge of  $9.7 \pm 12.0$ spikes/s was 4 times greater than on the flat surface (P = 0.004, t test; Fig. 7B4 and F4), constituting the group's main response to the ladder task, the vision processingrelated response.

In layer V, the activity of the 1-PEF group was unlike that in layers II–IV. It was strongly modulated with a peak at the time of the paw contact with the ladder and a dip in midswing (P = 0.01, U test; Fig. 7G2 and G4). This was different from this group activity on the flat surface when the peak was in swing (Fig. 7C2 and C4) and thus represented this group's response to the ladder task, a vision processing-related response. The discharge of 2-PEF noIDs in layer V at  $14.5 \pm 12.0$  spikes/s was 60% or  $\sim$ 5 spikes/s greater than on the flat surface (P = 0.006, t test). Their group activity had 2 subtle peaks: during stance-toswing transition and in the first half of stance (P = 0.01, U test; Fig. 7H2 and H4). The latter peak was this group's response to the ladder task, as it was absent on the flat surface (Fig. 7D2 and D4). It was 10% of the cycle later in the stride than the midcycle peak of 2-PEF noIDs in layers II-IV (Fig. 7F4) and was 15% later than the peak of 1-PEF noIDs in layer V (Fig. 7G4).

Across the 1-PEF and 2-PEF groups, the average dM of noIDs in layer V increased compared to the flat surface, from  $9.5 \pm 5.3$  to  $11.2 \pm 5.0$  (P = 0.006, t test), and was now similar to that of noIDs in layers II-IV, whose dM did not change upon transition to the ladder.

#### CCs

Example firing behavior of a low-active CC neuron during locomotion on the flat surface and the ladder is shown in Fig. 5F-J. While on the flat surface the neuron was practically silent, during 116 strides on the ladder it discharged 44 spikes, more than half of them compactly in midstance. Most others were fired at the end of swing. Thus, the activity of the neuron had 2 PEFs: a large one in midstance and a small one in late swing. The dM was high, 21.1, however, the peak discharge was only 2.5 spikes/s.

The activity of all 90 CC neurons tested during locomotion on the flat surface was tested on the ladder. The great majority were active: 93% (28/30) in cat 1 and 84% (50/60) in cat 2; 87% (78/90) across two cats. The average firing rate was as low as on the flat surface,  $2.7 \pm 3.9$ spikes/s. This was despite the increased activity of 30% (27/90) of the neurons, by  $3.7 \pm 3.9$  spikes/s on average, while the activity of only 8% (7/90) decreased. Proportions of cells increasing and decreasing activity were similar between layers II-IV and V (Fig. 4I and J). The value of the increase, however, was greater in layer V where the activity doubled, elevating to  $6.1 \pm 5.9$  spikes/s (P = 0.033, t test) and was now substantially higher than that of CCs in any other layer (P < 0.01, t test; Fig. 4B, dark gray bars).

Out of 78 neurons that were active on the ladder, only 62% (69% (62/90) of the entire CC population) discharged >1 spike. The discharge of all of these cells was modulated with the locomotion rhythm. The dM was  $15.7 \pm 6.7$ on average, which was similar to that on the flat surface and was significantly greater than in the noID group (P < 0.001, t test). Two main patterns of modulation were observed again, with 1 or 2 PEFs (Fig. 8C1 and C2 and D1 and D2). The 1-PEF pattern was still more common, expressed by 60% (37/62) of the cells, while 40% (25/62) had 2 PEFs. The proportion of 1-PEF CCs was similar to that on the flat surface, whereas that of 2-PEF cells tended to be larger (P=0.07,  $\chi^2$  test). The CC and noID populations with stride-related activity were similar in the proportions of neurons with 1-, 2-, and 3-PEF discharge patterns. The average duration of PEFs in the 1-PEF group was  $44\% \pm 23\%$  of the step cycle, whereas the combined duration of PEFs in the 2-PEF group was  $58\% \pm 11\%$ , 14% longer (P = 0.002, t test). As on the flat surface, the mean duration of the PEF among 1-PEF CCs was smaller by  $\sim$ 10% of the cycle than among noIDs (P = 0.02, t test), whereas the combined duration of PEFs in the 2-PEF CC and noID groups was similar.

The activity of the 1-PEF CC group was fairly steady across the step cycle at ~4 spikes/s (Fig. 8C4), which was similar to their behavior on the flat surface (Fig. 8A4). As on the flat surface, this steady discharge did not replicate the modulated activity of 1-PEF noIDs

(Fig. 8C4 vs. Fig. 6C4), nor did it reflect the change in the activity profile of noIDs upon transition to the ladder (Fig. 8A4 and C4 vs. Fig. 6A4 and C4).

The group discharge of 2-PEF CCs was modulated with the step cycle showing 2 peaks that were 10%–15% earlier in the cycle compared to those of 2-PEF noIDs (Fig. 8D4) vs. Fig. 6D4; to facilitate the comparison, in Fig. 8D4, the activity of noIDs is plotted as the light gray area graph in the background). Unlike on the flat surface, where 2-PEF CCs were less active than their 1-PEF counterparts, on the ladder, 2-PEF CCs were as active as 1-PEF CCs discharging  $5.3 \pm 5.4$  spikes/s (Fig. 8C4 and D4), which was 5 times more than on the flat surface (P = 0.001, t test; Fig. 8B4 and D4). This mirrored the behavior of the noID group, where 2-PEF cells were less active than 1-PEF ones on the flat surface but were as active as they on the ladder (Fig. 6B4 vs. A4 and Fig. 6D4 vs. C4). The activity of individual 2-PEF CCs was, however, less modulated than that of 1-PEF CCs, with the dM of  $12.4 \pm 3.4$  vs.  $17.9 \pm 7.5$ (P < 0.001, t test). This was now similar to 1-PEF and 2-PEF noIDs, between which the 2-PEF cells were always less modulated on average.

As during locomotion on the flat surface, the 1-PEF and 2-PEF CCs were equally distributed between layers II-IV and layer V. This was now similar to the equal distribution of 1-PEF and 2-PEF noIDs. In layers II-IV, the activity of 1-PEF CCs peaked at ~4 spikes/s in the beginning of swing, which was similar to their activity on the flat surface (Fig. 9E4 vs. A4). Thus, like 1-PEF noIDs in these layers (Fig. 7A4 and E4), layer II–IV CC group did not respond to the ladder task. The same was essentially true for the 2-PEF CC group in these layers whose discharge also peaked at ~4 spikes/s in the beginning of swing (Fig. 9F2 and F4) and was too largely similar to that on the flat surface (Fig. 9B2 and F4). This was in sharp contrast with the activity of 2-PEF noIDs in layers II-IV, which was dramatically different between flat surface and ladder locomotion (Fig. 7F4 vs. B4). Firing behavior of the fCC and sCC groups was similar in all these aspects.

In layer V, the activity of 1-PEF CCs was steady over the step cycle at ~5 spikes/s (Fig. 9G4). This was similar to their activity on the flat surface (Fig. 9C4) but was again sharply different from the modulated and substantially altered upon transition to the ladder activity of the 1-PEF noID group in this layer (Fig. 7G2 and G4 vs. C2 and C4). The only group of CCs, the activity of which was stride phase-modulated on the ladder, was layer V 2-PEF CCs. Their discharge was 3 times higher than on the flat surface (P = 0.03, t test) and fluctuated between 5 and 15 spikes/s in 2 waves that peaked 15% of the step cycle earlier compared to the peaks of layer V 2-PEF noIDs (Figs. 9H4 vs. 7H4; in Fig. 9H4, the activity of noIDs is shown by a light gray area graph in the background).

Across the 1-PEF and 2-PEF CC groups, the average dM of individual CCs in layers II-IV and V was similar, around 15, which was a greater magnitude compared to that of noIDs in either layer (P < 0.03, t test).

In summary, with the transition from visionindependent locomotion on the flat surface to visiondependent locomotion on the ladder:

- (i) The proportion of noIDs with stride-related activity rose from 87% to 98%, while that of CCs did not change, remaining much lower at 63%–69%. The proportion of 2-PEF noIDs almost doubled, while that of CCs had only a tendency to increase.
- (ii) In layers II-IV, the activity of the 2-PEF noID group rose 4-fold and became sharply modulated with peaks during the stance-to-swing and swing-to-stance transitions. By contrast, the group activity of 2-PEF CCs increased only slightly and in different phases of the stride, thus not reporting the noIDs' vision processingrelated activity to motor cortex. Both the 1-PEF noID and CC groups in layers II-VI did not respond to the ladder task.
- (iii) In layer V, the activity of the 1-PEF noID group became modulated with a peak during the swing-tostance transition and a dip during swing. The 1-PEF CC group did not respond to the ladder task, thus not reporting to motor cortex this vision processing-related activity of the 1-PEF noID group. The discharge of the 2-PEF noID group increased by 60% and became modulated with peaks during the stance-to-swing transition and in early stance. The 2-PEF CC group loudly forecasted this change to motor cortex 15% of the cycle earlier, or sent its own pronounced vision processing-related signal.

## Activity of neurons with somatosensory RFs on different segments of the forelimb or on the head

We earlier found that in motor cortex group activities of PTNs with RFs on different segments of the forelimb peak during different phases of the stride, suggesting distinct cortical control for the shoulder, elbow, and wrist (Stout and Beloozerova 2012; reviewed in Beloozerova et al. 2013). To evaluate whether area 5 neurons express any similar diversity and thus may contribute to the specificity of the cortical output addressed to different segments of the forelimb or the head, we grouped neurons according to the location of their somatosensory RF and compared their discharges.

#### noIDs

We found that groups of noIDs with RFs involving different body segments have different activity profiles during locomotion, both on the flat surface and the ladder. On the flat surface, the group activity of noIDs with an RF on the head (n = 9, from both layers II–IV and V) peaked during swing (P = 0.012, U test; Fig. 10A2 and A4). All but one neuron responded to the ladder task. The group average discharge slightly increased, but the activity profile did not change (Fig. 10E2 and E4).

The activity of the group of noIDs with an RF involving the shoulder (n = 32, all from layer V) on the flat surface peaked in early swing (P = 0.012, U test; Fig. 10B2 and B4), earlier in the cycle than that of the head-related cells. The overwhelming majority of neurons (88%, 28/32)

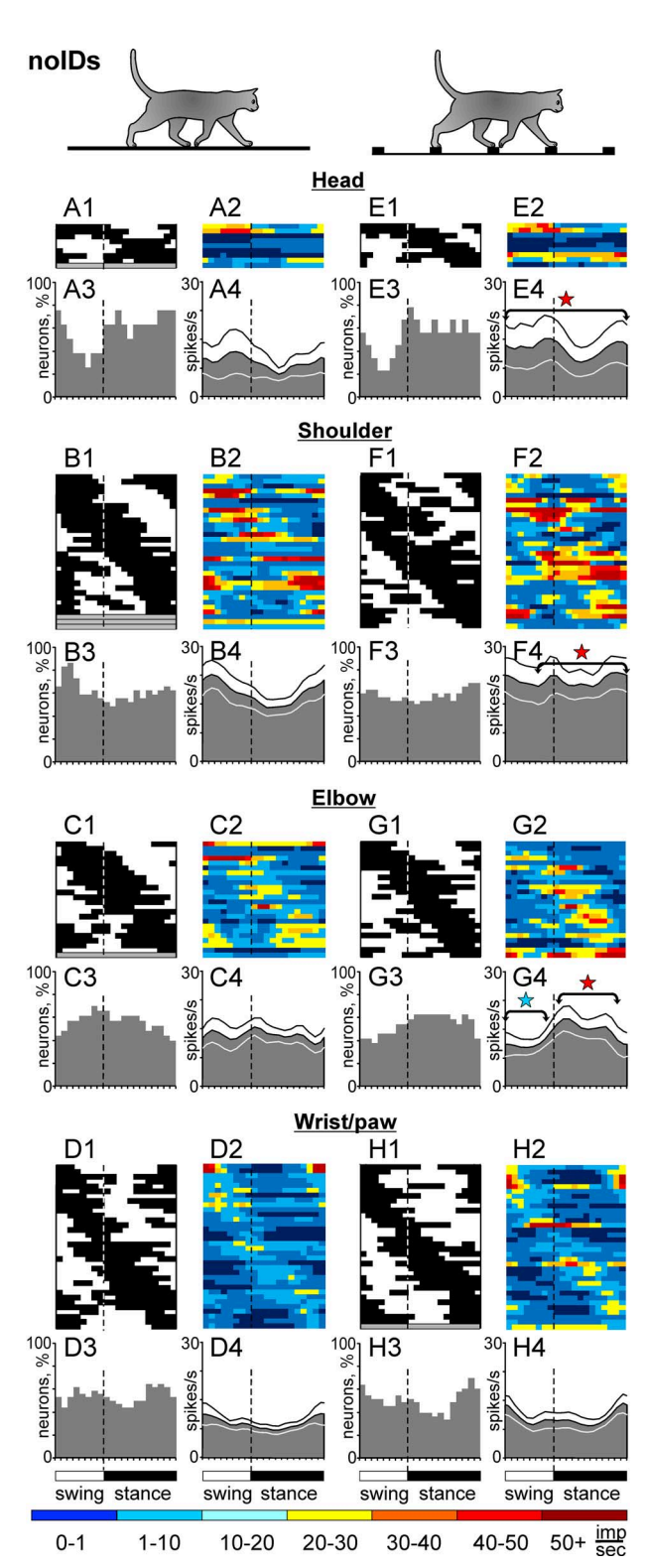


**Fig. 10.** noID neurons with somatosensory RFs on different segments of the forelimb and the head discharge during different phases of the stride. A, E) Activity of neurons with an RF on the head during flat surface (A) and ladder (E) locomotion. B, F) Activity of neurons with RFs involving the shoulder. C, G) Activity of neurons with RFs related to the elbow. D, H) Activity of neurons with RFs involving the wrist and/or paw. Gray bars in A1, B1, C1, and H1 designate neurons whose activity was not stride-modulated during given locomotor task. Other designations are as described in Figs. 6 and 7.

responded to the ladder task. The average discharge did not change, but the group activity profile lost its stride-related modulation (Fig. 10F2 and F4).

The activity of the elbow-related noID group (18 of 24 were in layer V) was fairly steady over the step cycle on the flat surface (Fig. 10C2 and C4). Most neurons (83%, 20/24) responded to the ladder, and the group activity became stride-modulated with a peak during stance (P = 0.012, U test; Fig. 10G2 and G4).

The group activity of noIDs with an RF on the wrist or paw (26 of 34 were in layer V) on the flat surface peaked during the stance-to-swing transition (P=0.012, U test; Fig. 10D2 and D4). Three-quarters of neurons (25/34) responded to the ladder task, however, the group activity profile did not change (Fig. 10 H2 and H4) and was still distinct from those of all other groups (Fig. 10E4, F4, and G4).

#### CCs

Although the number of active CCs in each of the shoulder-, elbow-, and wrist/paw-related groups was small, the results suggest that, similarly to noIDs, the activities of these CC groups during locomotion were distinct from each other.

CCs with RFs related to the shoulder (n=7) were located in both layers II-IV and V. They all had a fastconducting axon which projected to either MCprox, branched to MCprox and MCdist, or only projected to MCdist. On the flat surface, these neurons typically had a PEF during the stance-to-swing transition where the group activity peaked (P = 0.005, U test; Fig. 11A1 and A2). This activity profile was similar to that of the shoulderrelated noIDs, albeit the discharge rate was less than half of that of the noIDs (P = 0.04, t test; Fig. 10B4). However, the response of the shoulder-related CC group to the ladder task was different from that of the shoulderrelated noID group. Instead of losing its stride-related modulation, the discharge of this CC group became modulated with 2 peaks: one during the stance-to-swing transition, which was also present on the flat surface, and a new one during the swing-to-stance transition (P = 0.021, U test; Fig. 11E4).

The situation was different for the elbow-related cells. These CCs (n=6) were also found both in layers II–IV and V and had a fast-conducting axon projecting to either MCdist or MCprox. Similar to the shoulder-related CCs, their group activity on the flat surface peaked during swing (P=0.008, U test; Fig. 11B2 and B4). However, upon transition to the ladder, rather than forming a new peak during the swing-to-stance transition, the activity of this group still had only 1 peak during the stance-to-swing transition (P<0.001, U test; Fig. 11F4 vs. Fig. 11E4). The activity profiles of the elbow-related CCs were distinct from those of the elbow-related noIDs during both tasks (Fig. 10C4 and G4).

The activity of CCs with RFs on the wrist/paw (n=9) was different from that of either shoulder- or elbowrelated CC groups. These CCs were recorded from both

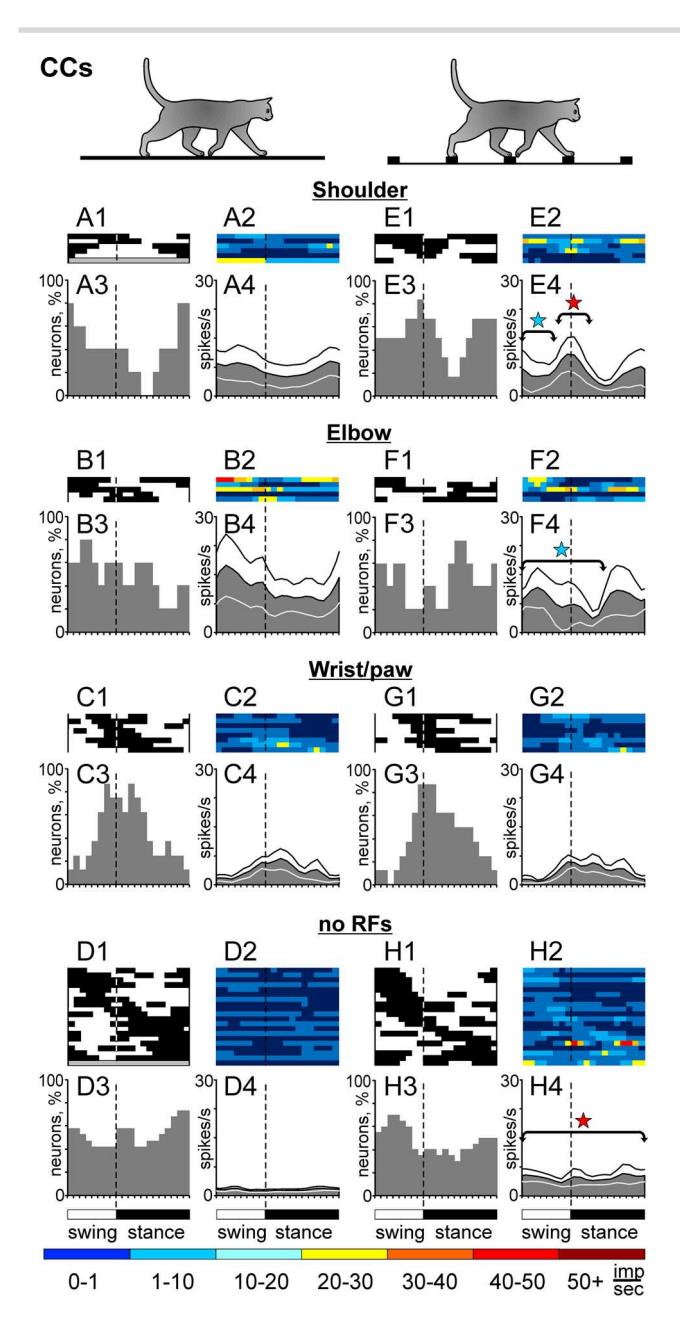


Fig. 11. CC neurons with somatosensory RFs on different segments of the forelimb discharge during different phases of the stride. The group activity of CCs without an RF is not stride-modulated. A, E) Activity of neurons with an RF involving the shoulder during flat surface (A) and ladder (E) locomotion. B, F) Activity of neurons with RFs related to the elbow. C, G) Activity of neurons with RFs involving the wrist and/or paw. D, H) Activity of neurons that did not respond to somatosensory or visual stimuli presented to the sitting animal. Designations are as described in Figs. 6, 7 and 10.

layers II-IV and V. They all projected to MCdist, and 6 of 9 were fCCs. On the flat surface, the group activity of the wrist/paw-related CCs peaked during the swingto-stance transition (P = 0.012, U test; Fig. 11C2 and C4). This was the opposite phase of the stride to that where the activity of both the shoulder- and elbow-related CC groups had their maxima (Fig. 11A4 and B4). Also, in sharp contrast to both the shoulder- and elbow-related CC groups, wrist/paw-related CCs as a group did not respond to the ladder task (Fig. 11G1-G4 vs. C1-C4). This

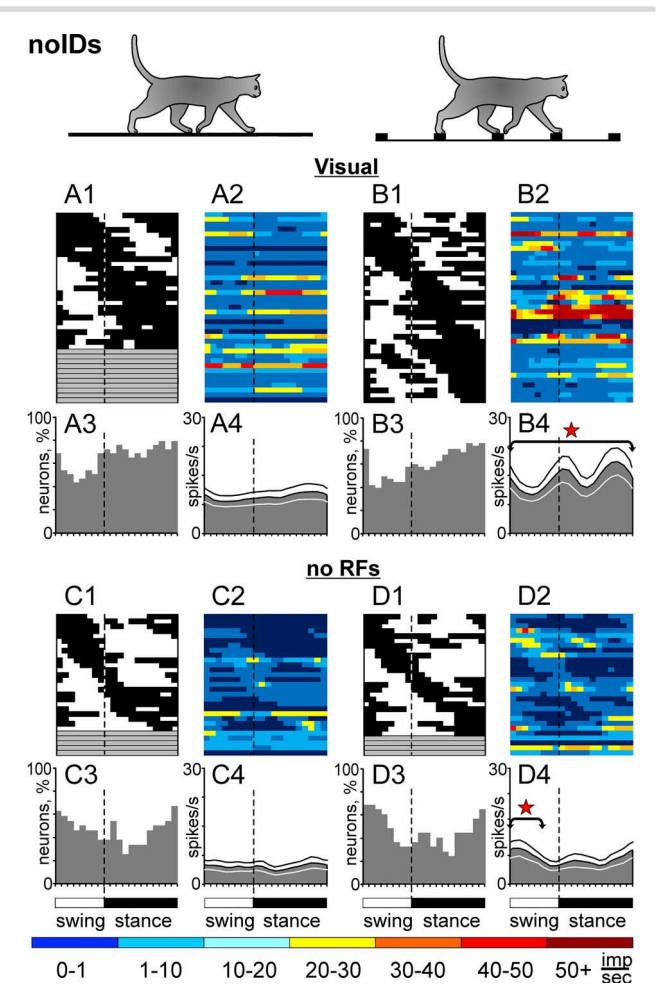


Fig. 12. Activity of noID neurons with a visual RF and those without either a somatosensory or visual RF. A, B) Neurons that responded to visual stimulation presented to the cat sitting with its head restrained. Activity during flat surface (A) and ladder (B) locomotion. C, D) Neurons that did not respond to visual or somatosensory stimulation in the sitting cat. Designations are as described in Fig. 6 and 10.

unresponsiveness to the ladder was analogous to that of the wrist/paw-related noID group (Fig. 10D1-D4 and H1-H4). However, the activity profile of the wrist/pawrelated CC group was distinct from that of the wrist/pawrelated noIDs during both tasks (Fig. 11C4 and G4 vs. 10D4 and H4).

Thus, like PTNs in motor cortex, groups of area 5 noIDs and CCs with somatosensory RFs on different segments of the forelimb have distinct activity profiles during both locomotion tasks. This suggests that they contribute to the specificity of the cortical output addressed to different forelimb segments. The activity profiles of CCs typically do not replicate those of noIDs.

## Activity of neurons with visual RF

Although the results of previous studies suggest that during locomotion area 5 is more involved in processing visual information and visuomotor transformations than in relaying the sensory visual information (Beloozerova and Sirota 2003; Marigold and Drew 2011), we felt that additional data on the role of sensory visual information in determining the stride-related modulation of the

activity of neurons in area 5 would be useful. Thus, we analyzed separately the activity of noIDs and CCs with visual RFs.

#### noIDs

Most visually responsive noIDs were found in layer V (64%, 25/39), while 28% (11/39) were in layers II-IV. In the sitting or standing cat, their average discharge was  $8.6 \pm 9.4$  spikes/s. With the start of locomotion on the flat surface, the discharge rate of 36% (14/39) of the neurons increased, by  $13.3 \pm 11.4$  spikes/s, while decreasing in 44% (17/39); the average discharge remained  $9.5 \pm 9.9$ spikes/s. The activity of 72% (28/39) of neurons was modulated with the locomotor rhythm: 56% (22/39) had 1 PEF and 15% (6/39) had 2. The average dM was  $6.5 \pm 5.6$ , much smaller than in the entire noID population (P < 0.001, t test). The group activity was steady over the step cycle (Fig. 12A2 and A4).

Upon transition to the ladder, the discharge of 38% (15/39) of the neurons increased, by  $11.6 \pm 8.5$  spikes/s, but the population's average still did not significantly change (14.0  $\pm$  15.3 spikes/s). All but 1 cell responded to the ladder task. The discharge of all was now modulated with the locomotor rhythm: 44% (17/39) had 1 PEF and 56% (22/39) had 2. The average dM was 8.7  $\pm$  4.7, which was similar to that on the flat surface and still much smaller than in the entire noID population (P = 0.002, t test). The activity profile of the population now had 2 peaks: during the swing-to-stance transition and at the end of stance (P=0.012, U test; Fig. 12B2 and B4). This profile was distinct from that of any group of noIDs with a somatosensory RF (Fig. 10).

#### CCs

The activity of only 5 CCs with a visual RF were tested during locomotion, and only 2 of them were active: a cell that responded to an object moving downward in front of the animal and a cell that responded to a grid moving to the right and an approaching object. The latter cell was also activated by passive flexion of the shoulder. Both cells had fast-conducting axons. On the flat surface, the activity of both was not stride-modulated. On the ladder, one cell discharged 1 PEF and another had 2 PEFs per stride. The 3 inactive CCs were all located in layers II–IV and had a fast-conducting axon projecting to MCdist.

Thus, all but 1 visually responsive noIDs responded to the ladder task, and the activity profile of the population dramatically changed. However, the average dM was lower than in the general noID population. These results suggest that during locomotion on the complex surface, the activity of area 5 noIDs may reflect both the sensory and processed visual information. The fact that 3 of 5 visually responsive CCs were inactive on the ladder indicates that the sensory visual information that reaches CCs is not the main cause of their locomotion-related activity on the complex surface and that transmitting this information to motor cortex is not the chief function of area 5 CCs.

## Activity of neurons without a somatosensory or visual RF

To further evaluate the importance of somatosensory and visual responsiveness for the stride-related activity modulation of the neurons, we analyzed separately the activity of noIDs and CCs that did not have a somatosensory or visual RF while the cat was sitting.

#### noIDs

Half of noIDs that did not have either a somatosensory or visual RF in the sitting animal (48%, 14/29) were located in layers II-IV. During locomotion on the flat surface, their activity was low,  $4.6 \pm 6.0$  spikes/s, lower than that of any other group of neurons with either a visual RF or a somatosensory RF on the forelimb (P < 0.03, t test). However, for 83% (24/29) of the neurons, this low-rate discharge was stride-modulated with a 1-PEF (15 cells), 2-PEF (8 cells), or 3-PEF (1 cell) pattern. The dM was  $13.7 \pm 9.0$ , which was similar to that of neurons with a somatosensory RF on the wrist/paw or elbow and was greater than that of cells with a somatosensory RF on the shoulder or head, or with a visual RF (P = 0.007, P = 0.034, P = 0.001, respectively, t test). The group activity was steady over the step cycle (Fig. 12C2 and C4). Upon transition to the ladder, 83% (24/29) of cells changed either the pattern of discharge or dM, and the group activity became step cycle-modulated with a peak in the early swing (Fig. 12D2 and D4). The average discharge of  $6.6 \pm 6.8$  spikes/s was still the lowest of the noID groups with either a visual RF or a somatosensory RF on the forelimb (P < 0.04, t test).

## CCs

Only slightly over a half of CCs without a somatosensory or visual RF whose activity was tested during locomotion (56%, 20/36) were active, which was substantially less than in the general CC population (P = 0.013,  $\chi^2$  test). Nine of the active cells were in layers II-IV, 8 were in layer V, and 3 were in layer VI. Eleven CCs had a fastconducting axon that all but 1 sent to MCdist, and 9 had a slow-conducting axon that could go to either MCdist or MCprox. Similar to the general CC population, the activity of these neurons on the flat surface was very low throughout the step cycle,  $1.5 \pm 1.4$  spikes/s (Fig. 11D2 and D4), less than half of that of noIDs without an RF. However, for all but 1 cells this lowrate discharge was stride phase-modulated with a 1-PEF (12 cells), 2-PEF (7 cells), or 3-PEF (1 cell) pattern. The dM was  $14.4 \pm 6.9$ , which was similar to that of CCs with a somatosensory or visual RF. Upon transition to the ladder, the group's average discharge increased to  $4.6 \pm 4.9$  spikes/s (P=0.01, t test; Fig. 11H2 and H4), becoming similar to that of the general CC population. Unlike for noIDs, the CC group activity remained steady over the step cycle; however, the discharge of individual neurons with an average dM of  $14.9 \pm 6.0$  was as modulated as that of CCs with a somatosensory or visual RF.

Collectively, the above results suggest that while the somatosensory and visual responsiveness of noID and CC neurons may elevate their mean discharge rates during locomotion, factors other than stimulation of somatosensory or visual RFs modulate their discharges in the rhythm of strides.

#### Discussion

We conducted experiments on cats because the activity of the general area 5 population during locomotion in cats has been described (e.g. Beloozerova and Sirota 2003; Andujar et al. 2010; Lajoie et al. 2010; Marigold and Drew 2011, 2017) as was the activity of motor cortex (e.g. Armstrong and Drew 1984a, 1984b; Drew 1988, 1993; Beloozerova and Sirota 1985, 1993a, 1993b; Beloozerova et al. 2010; Stout and Beloozerova 2012, 2013; Farrell et al. 2014, 2015). This assisted in considerations of how signals from area 5 may influence activity in motor cortex.

In this study, these considerations are mostly based on the comparison of the activity profiles of subpopulations of neurons subdivided by the layer position of their somata and the basic pattern of the stride-related activity modulation. One may wonder how important for successful locomotion on the ladder are the changes in the activity profile of a group of neurons containing quite diverse members, particularly with regard to the stride phase position of the PEF. We ultimately do not know whether it is the population average activity that is important for successful locomotion, or whether the activities of individual neurons are important. It is likely that they both contribute. We could see, however, that the profiles of population activities were quite robust with respect to which particular members were included in each population, as removing a randomly selected 1/4 of neurons from a group did not significantly change the profile of the group's activity, provided the group had ≥~20 members. This suggests that the activity profile of the subpopulations that we studied was a fair characteristic of these subpopulations. The discussion below is based on this assertion.

## Signals from area 5 to motor cortex during vision-independent locomotion on the flat surface—contribution of internal and peripheral information

We found that during vision-independent locomotion on the flat surface, the group activity of the broad area 5 neuronal populations (all cells, except those projecting to motor cortex in the rostral or lateral sigmoid gyrus) that discharged 1 or 2 bursts per stride peaked during different phases of the stride: the discharge of the 1-PEF group peaked during swing, whereas that of the 2-PEF group peaked during stance (Fig. 6A4 and B4). This difference was caused by the difference in the activity of these neuronal groups in cortical layer V, where the frequency of the discharge was much higher than in supragranular layers (Fig. 7C4 and D4 vs. A4 and B4). The

timing of the noID groups' maxima was not reported to motor cortex by the respective CC subpopulations, as the activities of these CC groups were largely steady over the step cycle (Figs. 8A4 and B4 and 9A4–D4). The activity of two-thirds of individual CCs, however, was step cycle-modulated, showing the same 1-PEF or 2-PEF patterns as individual noIDs. Although much fewer CCs were engaged in locomotion-related activity and their discharge rate was only 1/5th of that of noIDs (Fig. 4C-F), the ones that were active were transmitting to motor cortex stride-related signals 1 or 2 times per cycle. The dM was greater among CCs than noIDs, which means that CC signals to motor cortex were salient and therefore potentially impactful despite the low discharge rate.

Earlier it was suggested that the activation of somatosensory receptors does not importantly contribute to modulation of the activity of neurons in area 5 during locomotion on the flat surface (Beloozerova and Sirota 2003; Andujar et al. 2010). Results of the present study supported this view, as the activity of the great majority of noIDs without a somatosensory RF that could be detected in the sitting animal and the activity of more than a half of such CCs was, nevertheless, striderelated, suggesting that a source other than stimulation of somatosensory RFs influenced their discharges. In our 2003 report, we hypothesized that the 1-PEF pattern of the activity modulation of neurons in area 5 during locomotion on the flat surface reflects the 1-PEF activity pattern of neurons in the spinal locomotor central pattern generator (CPG; Beloozerova and Sirota 2003). This hypothesis was based on the similarity between the stride phase distributions of the activity of neurons in area 5 and spinal interneurons (Orlovsky and Feldman 1972; Baev et al. 1979; Viala et al. 1991; see also Musienko et al. 2020). Because the average separation of the two PEFs in the activity of 2-PEF neurons is close to 50% of the cycle, it is possible that the 2-PEF pattern of a subgroup of area 5 neurons reflects the activity of two, the left and right, locomotor CPGs.

Influenced by the spinal locomotor CPG or not, the activity of area 5 neuronal groups related to different segments of the forelimb is different. Discharge of the shoulder-related noIDs peaks in early swing (Fig. 10B4). The activity of the elbow-related noIDs is steady over the cycle (Fig. 10C4). Discharge of the wrist/paw-related noIDs has a weak maximum during the stance-toswing transition (Fig. 10D4). Although the number of tested CCs with a somatosensory RF on a specific segment of the forelimb was small, the activity of their groups also peaked in different phases of the stride (Fig. 11A4–C4). Interestingly, while the peak activation of the shoulder-related noID and CC groups coincided with the activity peak of the group of shoulder-related PTNs in motor cortex (Fig. 13A1–A3; Stout and Beloozerova 2012), the activity profiles of the elbow- and wrist/pawrelated noID and CC groups differed from those of the corresponding PTN groups (Fig. 13B1-B3 and C1-C3; Stout and Beloozerova 2012). This suggests that area 5

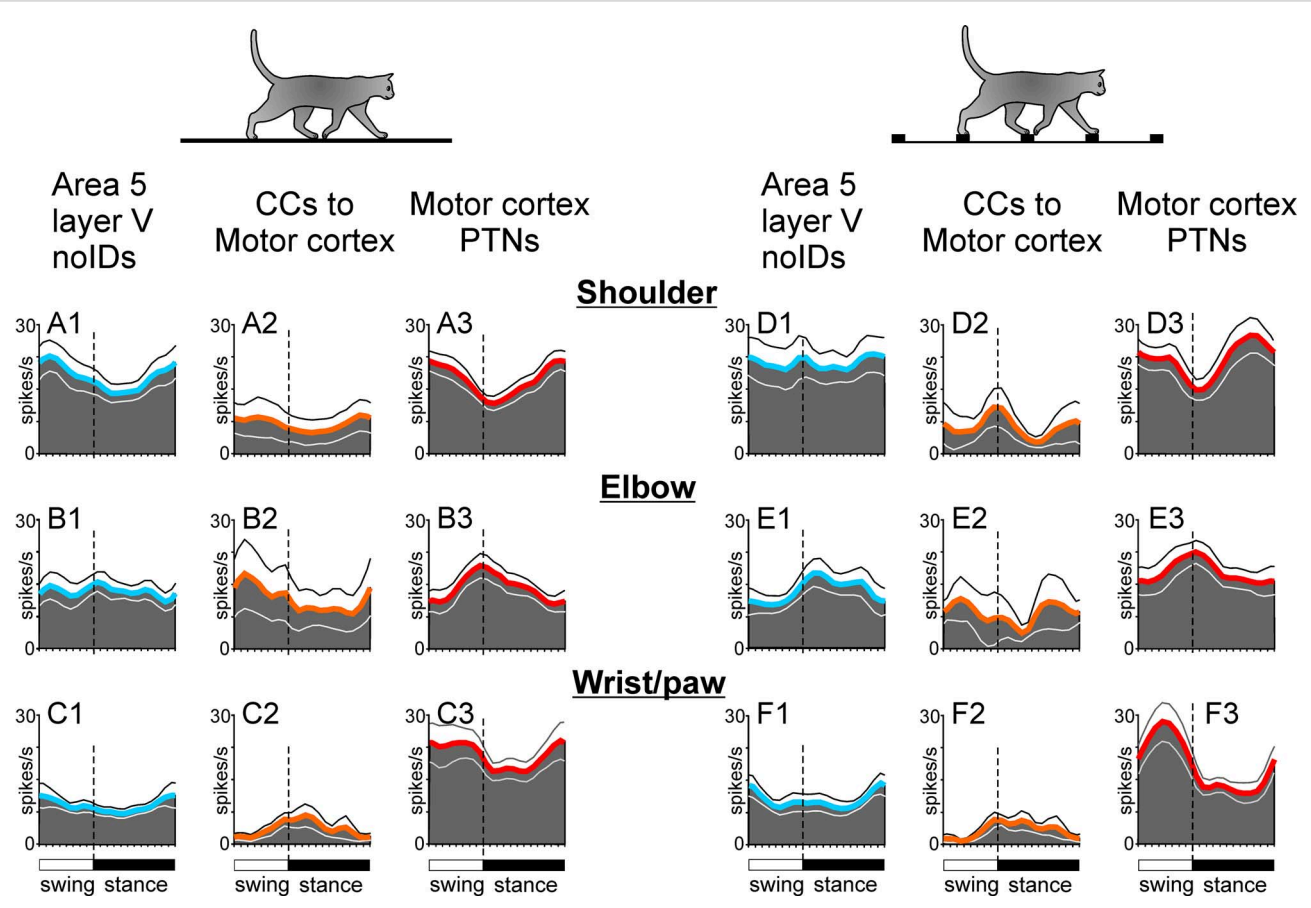


Fig. 13. Comparison of activity profiles of populations of shoulder-, elbow-, and wrist/paw-related neurons of area 5 (noIDs and CCs) and respective groups of pyramidal tract projection neurons (PTNs) of motor cortex. A–C) Group activity profiles of (A) shoulder-, (B) elbow-, and (C) wrist/paw-related neurons of area 5: noIDs (A1–C1, replotted from Fig. 10B4–D4) and CCs (A2–C2, replotted from Fig. 11A4–C4), and PTNs of motor cortex (A3–C3, modified from Figure 4H in Stout and Beloozerova 2012). D–F) Same for ladder locomotion: Fragments D1–F1 are replotted from Fig. 10F4–H4, fragments D2–F2 are replotted from Fig. 11E4–G4, and fragments D3–F3 are modified from Figure 7G in Stout and Beloozerova (2012). Designations are as described in Fig. 6.

influences the shoulder-, elbow-, and wrist/paw-related networks differently, including those located in motor cortex. Although limited, CC data suggest that most of this influence on motor cortex PTNs is not direct but is mediated, differently for different segments of the limb.

We have previously found that in the ventrolateral thalamus, which provides the main subcortical input to motor cortex, the activities of all 3 groups of neurons related to the 3 main segments of the forelimb: the shoulder, elbow, and wrist/paw, peak in the phases of the stride opposite to those where the activities of the corresponding PTN groups in motor cortex peak (Marlinski, Nilaweera, et al. 2012; Beloozerova et al. 2013). One of the explanations that we suggested was that these limb segment-specific groups of the ventrolateral thalamus influence their respective motor cortex PTNs via inhibitory interneurons in motor cortex (Beloozerova et al. 2013). In the Appendix, we consider whether the situation with the corticocortical input from area 5 may be similar, thus indicating a general principle of routing the basic locomotion movement-related information to PTNs of motor cortex via motor cortical inhibitory interneurons. It is worth noting that in the rabbit motor

cortex, corticofugal neurons of layer V and a subgroup of inhibitory interneurons are preferentially active in the opposite phases of the step cycle (Beloozerova et al. 2003). Also, in the mouse, it was recently found that the projection from the secondary to primary somatosensory cortex preferentially innervates inhibitory interneurons, and silencing this projection alters normal hind paw orientation during locomotion (Chang et al. 2022).

Signals from area 5 to motor cortex during vision-dependent locomotion on the ladder and their relation to gaze behavior—contribution of information about surface heterogeneity, time and distance to contact, precision of stepping, and direct visual input

In our earlier studies (Beloozerova and Sirota 1992, 2003), we found that during locomotion on a complex surface, parietal area 5 integrates visual information about the heterogeneity of the surface along the direction of locomotion with information about the activity of the basic locomotion mechanism and that the processed visual information dominates responses of its neurons. First, we found that when the cat has to overstep obstacles placed far apart, the discharges of area 5 neurons become

sharply modulated with the strides. However, when the distance between the obstacles decreases, increasingly restricting the space on the floor where the paws can step, thus making it more difficult for the cat to negotiate the obstacles, the activity of most neurons progressively loses its stride-related modulation (Beloozerova and Sirota 1992). Examples of such behavior of the neurons are shown in Supplementary Fig. 2. This demonstrates that during locomotion the discharge of many area 5 neurons is not related to the movement of the limbs and is not involved in the control of accuracy of locomotor movements but reflects the visual scene, which becomes progressively more homogenous as single far apart obstacles are replaced by densely spaced ones. In our later study, we found that when the cat walks along a narrow strip, a task that requires precise placing of paws on the support but on a pathway that is visually homogeneous along the direction of locomotion, the activity of area 5 neurons is similar to that on the flat surface (Beloozerova and Sirota 2003). Therefore, we concluded that the processed information about the visual heterogeneity of the surface along the direction of locomotion is the main factor that modulates the activity of area 5 neurons with the rhythm of strides on the complex surface. Later studies by the group of Dr Drew (Andujar et al. 2010) showed that while the activity of about half of area 5 neurons during stepping over a single obstacle correlates with the movement of a specific forelimb, that of another half is limb-independent and typically starts changing well before any limb steps over the obstacle. In the activity of 57% of the neurons, these changes persist in the dark, suggesting that area 5 is more involved in processing visual information needed to plan strides than in continual handling of sensory visual information (Marigold and Drew 2011). These findings extended our conclusion in that the visual information processed by area 5 may be used for planning stride adjustments. Marigold and Drew (2017) additionally found that there are dedicated subpopulations of neurons in area 5 that during an obstacle negotiation signal the distance to contact or time to contact with the obstacle, also highly processed information obtained by vision.

In our 2003 paper, we suggested that sensory visual information does not play much role in modulating the activity of neurons in area 5 during locomotion on the complex surface. This suggestion was put forward because even the highly sensitive to visual stimulation in the sitting animal neurons in the database considered in that study had lower discharge rates and striderelated modulation during locomotion on the ladder than neurons without visual RFs. The database considered here is different in that, although the stride-related modulation of the activity of its visually responsive noIDs on the ladder was too lower than that of cells without a visual RF, many of these noIDs responded to the ladder by increasing the discharge rate and the entire population changed the activity profile. This suggests that both sensory and processed visual information may influence

the activity of visually responsive cells in area 5 during locomotion on the complex surface.

To isolate the vision-related components in the activity of individual neurons and neuronal populations, we compared the activity of neurons between visionindependent locomotion on the flat surface and visiondependent locomotion on the ladder, specifically the ladder locomotion that has biomechanical characteristics close to those expressed on the flat surface. Locomotion along a horizontal ladder that has wide crosspieces placed at a distance of a typical length of the cat's stride provided a fitting comparison because (i) we have previously shown that, even when well-practiced, accurate stepping on such a ladder requires vision (Beloozerova and Sirota 2003) and (ii) we found that, out of 229 biomechanical variables of this locomotion, only a handful differ from those of locomotion on the flat surface (Beloozerova et al. 2010). These findings allowed us to interpret the differences in the activity of neurons observed between the flat surface and convenient ladder locomotion as a reflection of visual information processing during ladder locomotion. The probably increased attention during ladder locomotion may have contributed too, however, we do not think that it played the leading role in determining the striderelated responses of neurons on the ladder. At least for motor cortex, it was found that neuronal discharges during locomotion along a narrow strip are different from those observed on the ladder, while the level of required attention appeared to be comparable (Farrell et al. 2015). The situation for area 5 can be different, and a similar test should be conducted for this area as well; however, in the discussion below, we adopt a working hypothesis that the difference of the activity of area 5 neurons observed between flat surface and ladder locomotion chiefly reflects the processing of visual information.

Earlier, we analyzed gaze behavior of both cats used in this study while they performed the same locomotion tasks (Zubair et al. 2019). We found that during the step cycle, 4 gaze behaviors occur in a sequence two times each. At the beginning of a forelimb swing, the gaze shifts toward the cat along the walkway as a saccade (gaze shift toward [GST]; Fig. 14A). A third of the way into swing, GSTs peak and are then replaced by gaze fixations (FIX), which dominate the middle of the swing (Fig. 14B). During the last third of swing, gaze shifts away from the cat along the walkway occur, peaking at the time when the paw contacts the ladder's crosspiece (gaze shift away [GSA]; Fig. 14C). Finally, in the beginning of stance, during the forelimbs' double-support phase (illustrated, e.g. in Fig. 15 in Zubair et al. 2019), constant gaze is the dominant behavior (CG, Fig. 14D). This cycle then repeats with the start of the other forelimb's swing. Although the gaze in these cats was recorded not simultaneously with the activity of area 5 neurons, the fact that these were the same animals performing the same locomotion tasks in the same setting provides certain confidence in comparing the activity profiles of neuronal

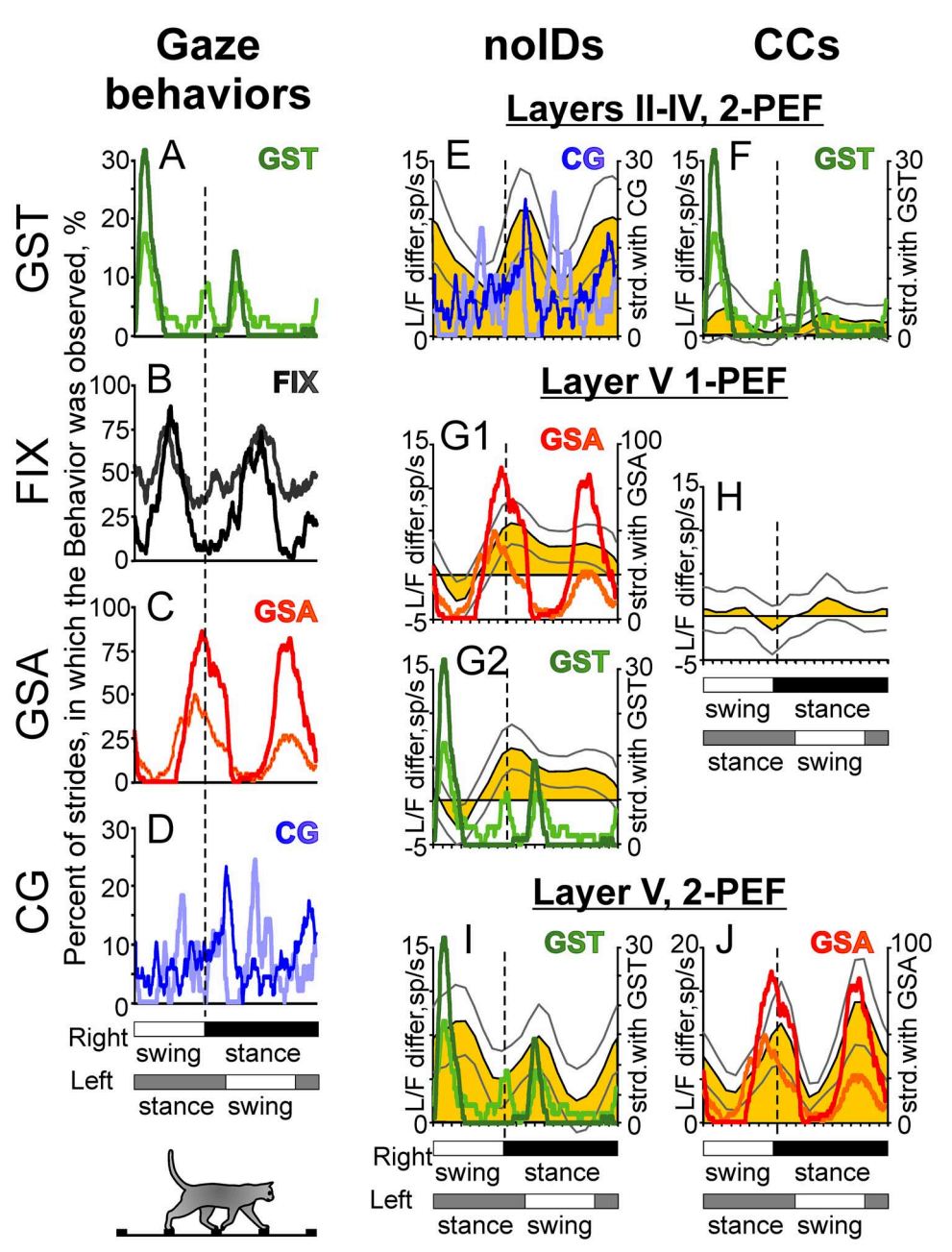


Fig. 14. Relationship of the vision-related component of the activity of noID and CC neurons in different cortical layers with 4 gaze behaviors. A-D) Frequency distributions of gaze behaviors in the step cycle of ladder locomotion obtained during one experiment with cat 1 (curves of light shade) and one experiment with cat 2 (curves of dark shade). Plots are adopted from Figures 14A, B of Zubair et al. (2019). A) Gaze shifts along the ladder toward the animal, GST. B) Gaze fixations on the ladder, FIX. C) Gaze shifts along the ladder away from the animal, GSA. D) Constant gaze along the ladder, CG. E-J) Relationship of the vision-related component of the activity of different groups of noID (E, G, and I) and CC (F, H, and J) neurons with the frequency distribution of gaze behaviors. In each fragment, the yellow area histogram depicts the bin-by-bin difference between the average activity of the group of neurons during flat surface and ladder locomotion, the vision-related component of the activity. Superimposed on the vision-related activity component are line graphs of the frequency distribution of a gaze behavior of the 2 cats which best matched the profile of the component. The scale on the left of each fragment is for the vision-related activity component, expressed in spikes/s, and the scale on the right is for the frequency of the gaze behavior, expressed in percent of strides, during which it was observed. E) The vision-related activity component of 2-PEF noIDs located in layers II-IV, plotted together with the frequency distribution histograms of constant gaze, CG. The vision-related activity component was calculated as the difference between the average discharge rates during flat surface and ladder locomotion plotted in Fig. 7B4 and F4. F) The vision-related activity component of 2-PEF CCs located in layers II-IV (the difference between activities of the group during the two tasks shown in Fig. 9B4 and F4), plotted together with the frequency distribution histograms of gaze shifts along the ladder toward the cat, GSTs. G1, G2) The vision-related activity component of 1-PEF noIDs of layer V (the difference between activities of the group in the two tasks shown in Fig. 7C4 and G4), plotted together with the frequency distribution histograms of gaze shifts along the ladder away from the animal, GSAs (G1) and toward the animal, GSTs (G2). H) The vision-related activity component of 1-PEF CCs of layer V was very small and did not match the frequency distribution of any gaze behavior. It was calculated as the difference between activities of the group in the two tasks shown in Fig. 9C4 and G4. I) The vision-related activity component of 2-PEF noIDs of layer V (the difference between activities of the group in the two tasks shown in Fig. 7D4 and H4), plotted together with the frequency distribution histograms of GSTs. J) The vision-related activity component of 2-PEF CCs of layer V (the difference between activities of the group in the two tasks shown in Figs. 9D4 and 7H4), plotted together with the frequency distribution histograms of GSAs. Other designations are as described in Fig. 6.

populations with the patterns of gaze behaviors. It is important to note that although upon transition from the vision-independent locomotion on the flat surface to the vision-dependent locomotion on the ladder cats slightly adjusted the timing of the gaze behaviors by making gaze fixations and gaze shifts away slightly earlier in the cycle, the pattern of gaze behaviors on the ladder was similar to that on the flat surface. This means that the difference in the relationship between the activity of neurons in area 5 and gaze behaviors during these two locomotor tasks chiefly reflects the difference in processing of visual information and not the difference in oculomotor behavior or head movement (for the pattern of head movement of these cats, see Zubair et al. 2016). Andujar et al. (2010) examined and did not find any consistent relationship between eye movements and the activity of area 5 neurons in the cat stepping over an obstacle.

Mirroring the sequence of gaze behaviors during the step cycle, there was a sequence of activation of different groups of area 5 neurons. To visualize the responses of neuronal groups to the ladder task and their relation to gaze behaviors, the difference between the activity of each group during flat surface and ladder locomotion is plotted as a yellow area histogram in Fig. 14E-J. As argued above, we consider this difference to represent the vision processing-related component of the activity of the neurons. Superimposed on this difference histogram are line graphs of a gaze behavior of the cats, replotted from Fig. 14A-D. For each neuronal group, a gaze behavior is shown, the frequency distribution of which best matches the profile of the vision-related activity component of the group. In Fig. 14E, one can see that the profile of this component of the group activity of 2-PEF noIDs in layers II-IV resembles the frequency distributions of constant gaze behavior, CG, both peaking during the first third of stance, the forelimbs' double-support phase. Constant gaze, also referred to as "travel fixation," occurs when a subject looks a fixed distance ahead during locomotion (Patla and Vickers 1997, 2003; Fowler and Sherk 2003) and the images of objects travel across the retina in a constant pattern. Results of many studies suggest that such "optic flow" provides useful information about both the objects in the environment and the subject's own movement (Gibson 1958; Lee 1980; Sun et al. 1992; Sherk and Fowler 2001). Subpopulations of neurons were recently found in area 5 that during locomotion on a complex surface signal distance to contact or time to contact with an obstacle, the two critical variables to take into account for avoiding one (Marigold and Drew 2017). Constant gaze simplifies the analysis of optic flow and the calculation of these variables. Because the vision-related activity component of 2-PEF noIDs of layers II-IV peaks during the 2 phases of the stride when constant gaze preferentially occurs, one can speculate that the activity of these neurons on the ladder reflects the processing of visual information obtained during constant gaze, including the distance to contact and time to contact with the ladder's

crosspiece. We did not see any group of CCs that, as a group, would discharge in synchrony with constant gaze and thus potentially relay information obtained from the optic flow during constant gaze to motor cortex; however, individual CCs that discharged in the beginning or end of stance could have relayed this information.

Next in the sequence are 1-PEF noIDs of layer V, the vision processing-related activity component of which peaks at the time of the paw/ladder contact, slightly lagging one of the peaks of gaze shifts away, GSAs (Fig. 14G1). Notably, this component has a negative trough in the first half of swing that slightly lags gaze shifts toward the cat, GSTs (Fig. 14G2). One may suggest that the visionrelated component of the activity of 1-PEF noIDs in layer V reflects the occurrence of gaze shifts as they pertain to the movement of the contralateral forelimb (see Fig. 15 in Zubair et al. 2019 for the relation of gaze behaviors to limb movements) while coding for the direction of the shift. Visual sampling is significantly suppressed during fast gaze shifts, the saccades (Bridgeman et al. 1975; reviewed in Wurtz 2008). Thus, an activity increase of 1-PEF noIDs in layer V at the time of the paw/ladder contact may warn their targets of a temporal gap in visual information during this phase and activate them in preparation for the information that will be obtained during the constant gaze immediately after. The depression of the activity of these noIDs in the first half of swing may advise their recipients of a temporal gap in visual information in this phase and disinhibit them in preparation for the information that will be obtained by gaze fixations immediately after. The neighboring 1-PEF CCs barely responded to the ladder (Fig. 14H), thus not transferring any of these signals to motor cortex. However, the neighboring 2-PEF CC group responded, showing an activity increase in synchrony with gaze shifts away while not having any activity reduction during gaze shifts toward (Fig. 14)). Importantly, their vision processing-related activity component corresponded to both peaks in gaze shifts away, the peaks related to the movement of the two, the right and left, forelimbs (Zubair et al. 2019).

Finally, the vision processing-related component of the activity of 2-PEF noIDs in layer V coincided with peaks in gaze shifts toward the cat, GSTs, which occur at the beginning of each forelimb's swing (Fig. 14I). Although sampling of visual information is suppressed during rapid gaze shifts in any direction, the CC group in this layer did not advise motor cortex about the lack of visual information in the beginning of swing. However, the vision-related activity component of the 2-PEF CC group in layers II-IV did have 2 small but statistically significant peaks that slightly lagged the peaks in gaze shifts toward (Fig. 14F).

We have recently shown that the acquisition of visual information during the stride on the ladder depends on the phase of the stride, and the extension of the phase window for the acquisition is closely related to the pattern of gaze behavior in cats (Volgushev et al. 2022).

Therefore, it is understandable that the area 5 processing of the periodically acquired visual information is also periodical and correlates with gaze behavior. The superposition of this processing upon the basic stride-related activity modulation observed during locomotion on the flat surface needs to be further investigated.

How is the activity of area 5 CCs during locomotion related to that of other CC populations? In a previous study conducted in the rabbit hopping on a flat surface or over obstacles, we characterized the activity of CCs of motor cortex (mCCs) projecting to the ipsilateral somatosensory cortex or contralateral motor or somatosensory cortex (Beloozerova et al. 2003). Like area 5 CCs, about half of mCCs were silent at rest, and the discharge rate of the active ones was quite low. However, unlike area 5 CCs, almost half of mCCs were still silent during locomotion, both on the flat surface and the ladder. The average discharge rate of the active CCs in the two cortices was similarly low, 2.4–4.4 spikes/s; however, the proportion of mCCs with the discharge modulated with the rhythm of strides was smaller, only 28% on the flat surface and 33% on the ladder (P < 0.001 for both,  $\chi^2$  test). This difference between CCs of area 5 and motor cortex shows that during locomotion, particularly locomotion on a complex surface that requires visuomotor coordination, more signals are sent from area 5 to motor cortex than from the motor cortex to somatosensory cortex or contralaterally. Unless this reflects an interspecies difference, this observation further supports the suggestion that on the complex surface signals from area 5 assist in the adjustment of strides based on the visual information.

## Area 5 participates in the differential control of the shoulder, elbow, and wrist/paw during vision-guided locomotion

Subpopulations of area 5 related to the shoulder, elbow, and wrist/paw responded differently to the ladder task, both noIDs and CCs. The shoulder-related noID and CC groups both increased activity during the swingto-stance transition (Fig. 13D1 and D2 vs. A1 and A2). This increase caused the discharge of the shoulderrelated noID group to become steady over the step cycle (Fig. 13D1), while for the CC group, it led to a development of a peak during this phase (Fig. 13D2). The situation was different for the elbow-related groups. Both noID and CC elbow-related populations changed their activity profiles upon transition to the ladder, and as the shoulderrelated groups, acted partly in unison; however, both reduced discharge during swing rather than increased it at the swing-to-stance transition. In addition, during stance, the noID group increased activity, while CCs decreased it (Fig. 13E1 and E2). Both responses were distinct from those of the corresponding shoulder-related groups. Still at variance, wrist/paw-related noIDs and CCs, as populations, both did not respond to the ladder task. Their group activity profiles were different but neither changed when the cat went from the flat surface

to the ladder (Fig. 13F1 and F2 vs. C1 and C2). Taken together, these observations suggest that, like motor cortex (Stout and Beloozerova 2012), somatosensory cortex (Favorov et al. 2015), and ventrolateral thalamus (Marlinski, Nilaweera, et al. 2012; Marlinski, Sirota, et al. 2012; Marlinski and Beloozerova 2014; Beloozerova et al. 2013), area 5 differentially controls the shoulder, elbow, and wrist/paw during vision-guided locomotion.

There were a number of hypotheses proposed for the role of area 5 in the control of limb movements, including the "sensory" hypothesis (Hyvarinen 1982), the "command" hypothesis (Mountcastle et al. 1975), the "planning action" hypothesis (Andersen et al. 1998), the "attention" hypothesis (Colby and Goldberg 1999), the "decision" hypothesis (Shadlen and Newsome 2001), the "reference frames transformation" hypothesis (Cohen and Andersen 2002), the "working memory" hypothesis (Wong and Lomber 2019), and others. As noted long ago by Dr Kalaska (1996) and touched upon in the discussion above, the diverse roles of area 5 may be complementary to each other. Such complementarity can be achieved by the concurrent activity of different subpopulations of neurons such as those located in different cortical layers and related to the movement of one or both forelimbs, or to different segments of a limb.

## Conclusion

We have analyzed for the first time the signals that are transmitted by CCs of area 5 to motor cortex during behavior. We studied locomotion because this is the most basic, defining, behavior of all animals. Comparing neuronal activity during vision-dependent and visionindependent locomotion tasks allowed us to isolate the components of the activity that are related to the processing of visual information during locomotion on the complex surface. We found that groups of area 5 CCs largely do not replicate the activity of the neighboring broad populations but transmit their own signals to motor cortex. These signals appear to be specific to particular segments of the forelimb. They coincide with peaks of gaze shifts along the walking path. The group activation of different noID subpopulations also peaks together with gaze shifts, and in addition, 2-PEF noIDs of layers II-IV are active during the phase of the stride when constant gaze dominates, a behavior during which visual information from optic flow can be effectively collected. This latter information is not transmitted to motor cortex by coherent activity of any CC group that we studied. The phase-related inferences with gaze behaviors that we make, while speculative, build a framework for further experiments that will determine the working relationship between the activity of area 5 neurons, gaze behavior, and vision and will ultimately reveal how visual information that arrives to motor cortex via the dorsal stream influences motor commands dispatched from motor cortex to the spinal cord to accurately guide limbs to objects.

## **Authors' contributions**

I.N.B. conceived and designed the research, prepared the figures, and drafted the manuscript. I.N.B., W.U.N., G.V.D.P., and V.M. performed the experiments, analyzed the data, edited and revised the manuscript, and approved the final version of the manuscript. I.N.B., W.U.N., and V.M. interpreted the results of experiments.

# **Acknowledgements**

The authors are indebted to Mr Peter Wettenstein for his exceptional engineering assistance.

# Supplementary material

Supplementary material is available at Cerebral Cortex Journal online.

# **Funding**

This research was supported by National Science Foundation (grant 1912557) to I.N.B., and in part, by the National Institute of Neurological Disorders and Stroke (grant R01 NS-058659) to I.N.B.

Conflict of interest statement. None declared.

# Data availability

The data supporting the findings of this study are available from the corresponding author (I.N.B., ibeloozerova3@gatech.edu) upon request.

## **Abbreviations**

CC, corticocortical neuron projecting axon from area 5 to ipsilateral motor cortex

dM, coefficient of stride-related activity modulation, the "depth" of modulation.

fCC, corticocortical neuron with a fast-conducting axon. MCdist, representation of the distal forelimb in motor

MCprox, representation of the proximal forelimb in motor cortex.

noID, neuron with a nonidentified projection of the axon. PEF, period of elevated firing.

PTN, pyramidal tract projection neuron.

RF, receptive field.

sCC, corticocortical neuron with a slow-conducting axon.

## **Definitions**

Peripheral (sensory) visual information, information that the neuron receives from stimulation of its visual RF. Processed visual information, information that the neuron receives from other sources that results from the analysis (processing) of sensory information. This includes information about the structure of the walking pathway, the distance and the time to contact with an obstacle.

Visual heterogeneity, the nonuniform structure of the distribution of visual contrast in the environment. The information about visual heterogeneity of the walking surface is a type of processed visual information.

Visual information, peripheral (sensory) and processed visual information referred to jointly.

# Appendix. Signals from area 5 to motor cortex are limb segment-specific and appear to influence PTNs of motor cortex via inhibitory interneurons

Although only a small sample of CCs with somatosensory RFs on a specific segment of the forelimb was tested during locomotion (Table 1), the results suggest that, similarly to area 5 populations projecting elsewhere, area 5 CCs projecting to motor cortex influence the shoulder-, elbow- and wrist/paw-related networks in the motor cortex differently.

During locomotion on the flat surface, the activity of the shoulder-related CC group, almost all cells of which projected to MCprox, the shoulder-related area in motor cortex, peaked during the stance-to-swing transition (Fig. 11A4). The activity of the elbow-related group, whose neurons could project either to MCprox or MCdist, peaked during swing (Fig. 11B4). Still at variance, the discharge of the wrist/paw-related CCs, all of which projected to MCdist, was maximal during swing-to-stance transition (Fig. 11C4). Whereas the peak activation of the shoulder-related CC group coincided with the activity peak of shoulder-related PTNs in motor cortex (Fig. 13A2 and A3; Stout and Beloozerova 2012), the activity of the elbow- and wrist/paw-related CCs groups peaked in different phases compared to the corresponding PTN groups. Moreover, the activity of the elbow-related CC group was maximal in the early swing when the activity of elbow-related PTNs in motor cortex dips (Fig. 13B2 and B3). Likewise, the activity of wrist/paw-related CCs was maximal when the discharge of the respective PTNs in motor cortex is at its minimum (Fig. 13C2 and C3). During locomotion on the ladder, the activity profiles of the shoulder-, elbow- and wrist/pawrelated CC groups were all different as well (Fig. D2-F2), and now each of them peaked in an opposite phase of the stride compared to where the corresponding PTN group of motor cortex had its activity maximum (Fig. D3-F3).

These data suggest that during vision-independent locomotion on the flat surface, the influence from area 5 on the shoulder-related networks in motor cortex goes directly to its output elements, the PTNs, while that on the elbow- and wrist/paw-related networks targets inhibitory interneurons in motor cortex. During locomotion on the ladder, which requires accurate visually guided stepping, the shoulder-related CC signals appear to reach PTNs via inhibitory interneurons as well. If true, this would be similar to how the main subcortical input to motor cortex, the one from the ventrolateral thalamus, appears to influence the networks related to different segments of the forelimb in motor cortex (Marlinski, Nilaweera, et al. 2012; Beloozerova et al. 2013).

## References

- Andersen RA, Cui H. Intention, action planning, and decision making in parietal-frontal circuits. Neuron. 2009:63(5):568-583.
- Andersen RA, Snyder LH, Bradley DC, Xing J. Multimodal representation of space in the posterior parietal cortex and its use in planning movements. Annu Rev Neurosci. 1997:20:303-330.
- Andersen RA, Snyder LH, Batista AP, Buneo CA, Cohen YE. Posterior parietal areas specialized for eye movements (LIP) and reach (PRR) using a common coordinate frame. Novartis Found Symp. 1998:218:109-122.
- Andujar JE, Drew T. Organization of the projections from the posterior parietal cortex to the rostral and caudal regions of the motor cortex of the cat. J Comp Neurol. 2007:504(1):17-41.
- Andujar JE, Lajoie K, Drew T. A contribution of area 5 of the posterior parietal cortex to the planning of visually guided locomotion: limb-specific and limb-independent effects. J Neurophysiol. 2010:103(2):986-1006.
- Armer MC, Nilaweera WU, Rivers TJ, Dasgupta NM, Beloozerova IN. Effect of light on the activity of motor cortex during locomotion. Behav Brain Res. 2013:250:238-250.
- Armstrong DM, Drew T. Discharges of pyramidal tract and other motor cortical neurons during locomotion in the cat. J Physiol Lond. 1984a:346:471-495.
- Armstrong DM, Drew T. Locomotor-related neuronal discharges in cat motor cortex compared with peripheral receptive fields and evoked movements. J Physiol Lond. 1984b:346:497-517.
- Armstrong DM, Drew T. Topographical localization in the motor cortex of the cat for somatic afferent responses and evoked movements. J Physiol Lond. 1984c:350:33-54.
- Armstrong DM, Drew T. Electromyographic responses evoked in muscles of the forelimb by intracortical stimulation in the cat. J Physiol Lond. 1985:367:309-326.
- Asanuma H. The pyramidal tract. In: Brookhart JM, Mountcastle VB, Brooks VB, editors. Handbook of physiology. sect 1. Vol. II. Bethesda (MD): Am Physiol Soc; 1981. pp. 703-733
- Avendano C, Rausell E, Reinoso-Suarez F. Thalamic projections to areas 5a and 5b of the parietal cortex in the cat: a retrograde horseradish peroxidase study. J Neurosci. 1985:5(6):1446-1470.
- Avendano C, Rausell E, Perez-Aguilar D, Isorna S. Organization of the association cortical afferent connections of area 5: a retrograde tracer study in the cat. J Comp Neurol. 1988:278(1):1-33.
- Babb RS, Waters RS, Asanuma H. Corticocortical connections to the motor cortex from the posterior parietal lobe (areas 5a, 5b, 7) in the cat demonstrated by the retrograde axonal transport of horseradish peroxidase. Exp Brain Res. 1984:54:476-484.
- Baev KV, Degtiarenko AM, Zavadskaia TV, Kostiuk PG. Activity of interneurons of the lumbar region of the spinal cord during fictive locomotion of thalamic cats (in Russian). Neirofiziologiia. 1979:11:329-338.
- Batshelet E. Circular statistics in biology. London: Academic Press; 1981 Batuev AS, Cherenkova LV, Yunatov YA. Association brain systems and visually guided movements in the cat. Physiol Behav. 1983:31(1):29-38.
- Beloozerova IN, Marlinski V. Contribution of the ventrolateral thalamus to the locomotion-related activity of motor cortex. J Neurophysiol. 2020:124(5):1480-1504.

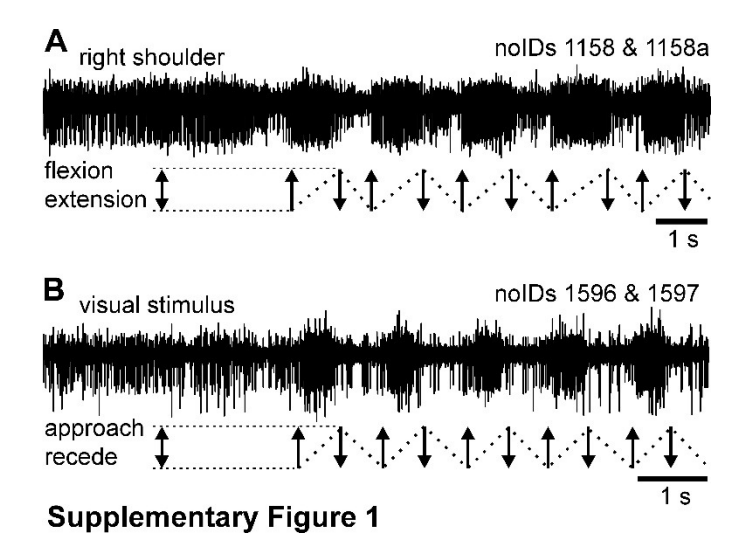
- Beloozerova IN, Sirota MG. Activity of neurons of the motosensory cortex during natural locomotion in the cat. Neirofiziologiia. 1985:17(3):406-408 Article in Russian.
- Beloozerova IN, Sirota MG. The role of motor cortex in control of locomotion. In: Gurfincel VS, Ioffe ME, Massion J, Roll JP, editors. Stance and motion. Facts and concepts. New York: Plenum press; 1988. pp. 163-176
- Beloozerova IN, Sirota MG. Activity of neurons in area 5 of the cerebral cortex during locomotion in awake cats. J Physiol Lond. 1992:45:291P.
- Beloozerova IN, Sirota MG. The role of the motor cortex in the control of accuracy of locomotor movements in the cat. J Physiol Lond. 1993a·461·1-25
- Beloozerova IN, Sirota MG. The role of the motor cortex in the control of vigour of locomotor movements in the cat. J Physiol Lond. 1993b:461:27-46.
- Beloozerova IN, Sirota MG. Integration of motor and visual information in the parietal area 5 during locomotion. J Neurophysiol. 2003:90:961-971.
- Beloozerova IN, Sirota MG, Swadlow HA. Activity of different classes of neurons of the motor cortex during locomotion. J Neurosci. 2003:23(3):1087-1097.
- Beloozerova IN, Farrell BJ, Sirota MG, Prilutsky BI. Differences in movement mechanics, electromyographic, and motor cortex activity between accurate and non-accurate stepping. J Neurophysiol. 2010:103:2285-2300.
- Beloozerova IN, Stout EE, Sirota MG. Distinct thalamo-cortical controls for shoulder, elbow, and wrist during locomotion. Front Comput Neurosci. 2013:21(7):62.
- Bishop PO, Burke W, Davis R. The identification of single units in central visual pathways. J Physiol Lond. 1962:162:409-431.
- Bridgeman B, Hendry D, Stark L. Failure to detect displacement of the visual world during saccadic eye movements. Vis Res. 1975:15: 719-722.
- Chambers WWV, Liu CN. Corticospinal tract of the cat. An attempt to correlate the pattern of degeneration with deficit in reflex act following neocortical lesions. J Comp Neurol. 1957:108:23-26.
- Chang C-W, Zhao M, Grudzien S, Oginsky M, Yang Y, Kwon SE. A cortico-cortical pathway targets inhibitory interneurons and modulates paw movement during locomotion in mice. J Neurosci. 2022:42(1):44-57.
- Cohen YE, Andersen RA. A common reference frame for movement plans in the posterior parietal cortex. Nat Rev Neurosci. 2002:3: 553-562.
- Colby CL, Goldberg ME. Space and attention in parietal cortex. Annu Rev Neurosci. 1999:22:319-349.
- de Carvalho WD, Rosalino LM, Dalponte JC, Santos B, Harumi Adania C, Lustosa Esbérard CE. Can footprints of small and medium sized felids be distinguished in the field? Evidences from Brazil's Atlantic Forest. Trop Conserv Sci. 2015:8(3):760-777.
- Drew T. Motor cortical cell discharge during voluntary gait modification. Brain Res. 1988:457(1):181-187.
- Drew T. Motor cortical activity during voluntary gait modifications in the cat. I. Cells related to the forelimbs. J Neurophysiol. 1993:70:
- Drew T, Doucet S. Application of circular statistics to the study of neuronal discharge during locomotion. J Neurosci Methods. 1991:38:171-181.
- Efron B, Tibshirani RJ. An introduction to the bootstrap. New York: Chapman & Hall; 1993
- Fabre M, Buser P. Structures involved in acquisition and performance of visually guided movements in the cat. Acta Neurobiol Exp. 1980:40:95-116.

- Fabre M, Buser P. Effect of lesioning the anterior suprasylvian cortex on visuo-motor guidance performance in the cat. Exp Brain Res. 1981-41-81-88
- Farr TD, Liu L, Colwell KL, Whishaw IQ, Metz GA. Bilateral alteration in stepping pattern after unilateral motor cortex injury: a new test strategy for analysis of skilled limb movements in neurological mouse models. J Neurosci Methods. 2006:153(1):104-113.
- Farrell BJ, Bulgakova MA, Beloozerova IN, Sirota MG, Prilutsky BI. Body stability and muscle and motor cortex activity during walking with wide stance. J Neurophysiol. 2014:112(3):504-524.
- Farrell BJ, Bulgakova MA, Sirota MG, Prilutsky BI, Beloozerova IN. Accurate stepping on a narrow path: mechanics, EMG, and motor cortex activity in the cat. J Neurophysiol. 2015:114(5): 2682-2702.
- Favorov OV, Nilaweera WU, Miasnikov AA, Beloozerova IN. Activity of somatosensory responsive neurons in high subdivisions of SI cortex during locomotion. J Neurosci. 2015:35(20):7763-7776.
- Fisher NI. Statistical analysis of circular data. Cambridge: Cambridge University Press; 1993
- Fowler GA, Sherk HA. Gaze during visually guided locomotion in cats. Behav Brain Res. 2003:139:83-96.
- Friel KM, Drew T, Martin JH. Differential activity-dependent development of corticospinal control of movement and final limb position during visually guided locomotion. J Neurophysiol. 2007:97: 3396-3406.
- Fuller JH, Schlag JD. Determination of antidromic excitation by the collision test: problems of interpretation. Brain Res. 1976:112: 283-298
- Gallivan JP, Goodale MA. The dorsal "action" pathway. Handb Clin Neurol. 2018:151:449-466.
- Gamberini M, Passarelli L, Fattori P, Galletti C. Structural connectivity and functional properties of the macaque superior parietal lobule. Brain Struct Funct. 2020:225(4):1349-1367.
- Ghosh S. Cytoarchitecture of sensorimotor areas in the cat cerebral cortex. J Comp Neurol. 1997a:388:354-370.
- Ghosh S. Comparison of the cortical connections of areas  $4\gamma$  and  $4\delta$ in the cat cerebral cortex. J Comp Neurol. 1997b:388:371-396.
- Gibson JJ. Visually controlled locomotion and visual orientation in animals. Br J Psychol. 1958:49:182-194.
- Goodale MA, Milner AD. Separate visual pathways for perception and action. Trends Neurosci. 1992:15:20-25.
- Groos WP, Ewing LK, Carter CM, Coulter JD. Organization of corticospinal neurons in the cat. Brain Res. 1978:143:393-341.
- Hassler R, Muhs-Clement K. Architektonischer Aufbau des sensomotorischen und parietalen Cortex der Katze. J Hirnforsch. 1964:6:
- Hentall ID, Zorman G, Kansky S, Fields HL. Relations among threshold, spike height, electrode distance, and conduction velocity in electrical stimulation of certain medullospinal neurons. J Neurophysiol. 1984:51:968-977.
- Hyvarinen J. The parietal cortex of monkey and man. Studies of brain function. Vol. 8. Berlin, Heidelberg: Springer-Verlag; 1982
- Kakei S, Futami T, Shinoda Y. Projection pattern of single corticocortical fibers from the parietal cortex to the motor cortex. Neuroreport. 1996:7:2369-2372.
- Kalaska JF. Parietal cortex area 5 and visuomotor behavior. Can J Physiol Pharmacol. 1996:74:483-498.
- Lajoie K, Drew T. Lesions of area 5 of the posterior parietal cortex in the cat produce errors in the accuracy of paw placement during visually guided locomotion. J Neurophysiol. 2007:97(3):2339-2354.
- Lajoie K, Andujar JE, Pearson K, Drew T. Neurons in area 5 of the posterior parietal cortex in the cat contribute to interlimb

- coordination during visually guided locomotion: a role in working memory. J Neurophysiol. 2010:103(4):2234-2254.
- Lee DN. The optic flow field: the foundation of vision. Philos Trans R Soc Lond Ser B Biol Sci. 1980:290:169–179.
- Leichnetz GR, Smith DJ, Spencer RF. Cortical projections to the paramedian tegmental and basilar pons in the monkey. J Comp Neurol. 1984:228:388-408.
- Liddell EGT, Phillips CG. Pyramidal section in the cat. Brain. 1944:67:
- Marigold DS, Drew T. Contribution of cells in the posterior parietal cortex to the planning of visually guided locomotion in the cat: effects of temporary visual interruption. J Neurophysiol. 2011:105(5):2457-2470.
- Marigold DS, Drew T. Posterior parietal cortex estimates the relationship between object and body location during locomotion. elife. 2017:6:pii: e28143.
- Marlinski V, Beloozerova IN. Burst firing of neurons in the thalamic reticular nucleus during locomotion. J Neurophysiol. 2014:112(1): 181-192.
- Marlinski V, Nilaweera WU, Zelenin PV, Sirota MG, Beloozerova IN. Signals from the ventrolateral thalamus to the motor cortex during locomotion. J Neurophysiol. 2012:107:455-472.
- Marlinski V, Sirota MG, Beloozerova IN. Differential gating of thalamo-cortical signals by reticular nucleus of thalamus during locomotion. J Neurosci. 2012:32(45):15823-15836.
- Martin JH, Ghez C. Differential impairments in reaching and grasping produced by local inactivation within the forelimb representation of the motor cortex in the cat. Exp Brain Res. 1993:94:429-443.
- Metz GA, Whishaw IQ. Cortical and subcortical lesions impair skilled walking in the ladder rung walking test: a new task to evaluate fore- and hindlimb stepping, placing, and co-ordination. J Neurosci Methods. 2002:115:169-179.
- Mountcastle VB. The parietal system and some higher brain functions. Cereb Cortex. 1995:5(5):377-390.
- Mountcastle VB, Lynch JC, Georgopoulos A, Sakata H, Acuna C. Posterior parietal association cortex of the monkey: command functions for operations within extrapersonal space. J Neurophysiol. 1975:38:871-908.
- Murray EA, Coulter JD. Organization of corticospinal neurons in the monkey. J Comp Neurol. 1981:195:339-365.
- Musienko PE, Lyalka VF, Gorskii OV, Merkulyeva N, Gerasimenko YP, Deliagina TG, Zelenin PV. Comparison of operation of spinal locomotor networks activated by supraspinal commands and by epidural stimulation of the spinal cord in cats. J Physiol. 2020:598(16):3459-3483.
- Nieoullon A, Rispal-Padel L. Somatotopic localization in cat motor cortex. Brain Res. 1976:105:405-422.
- Orlovsky GN, Feldman AG. Classification of lumbosacral neurons according to their discharges during evoked locomotion (in Russian). Neurophysiologia. 1972:4:410-417.
- Patla AE, Vickers JN. Where and when do we look as we approach and step over an obstacle in the travel path? Neuroreport. 1997:8: 3661-3665.
- Patla AE, Vickers JN. How far ahead do we look when required to step on specific locations in the travel path during locomotion? Exp Brain Res. 2003:148:133-138.
- Phillips CG, Porter R. Corticospinal neurons. Their role in movement. Monogr Physiol Soc. 1977:v-xii(34):1-450.
- Prilutsky BI, Sirota MG, Gregor RJ, Beloozerova IN. Quantification of motor cortex activity and full-body biomechanics during unconstrained locomotion. J Neurophysiol. 2005:94:2959-2969.
- Pryor K. Lads before the wind. New York: Harper and Row; 1975.

- Rathelot JA, Dum RP, Strick PL. Posterior parietal cortex contains a command apparatus for hand movements. Proc Natl Acad Sci U S A. 2017:114(16):4255–4260.
- Rivers TJ, Sirota MG, Guttentag AI, Ogorodnikov DA, Shah NA, Beloozerova IN. Gaze shifts and fixations dominate gaze behavior of walking cats. Neuroscience. 2014:275:477–499.
- Rondot P, de Recondo J, Dumas JL. Visuomotor ataxia. *Brain.* 1977:100: 355–376.
- Shadlen MN, Newsome WT. Neural basis of a perceptual decision in the parietal cortex (area LIP) of the rhesus monkey. *J Neurophysiol*. 2001:86:1916–1936.
- Sherk H. Visual response properties of cortical inputs to an extrastriate cortical area in the cat. Vis Neurosci. 1989:3(3):249–265.
- Sherk H. Functional organization of input from areas 17 and 18 to an extrastriate area in the cat. *J Neurosci*. 1990:10(8):2780–2790.
- Sherk H, Fowler GA. Neural analysis of visual information during locomotion. Prog Brain Res. 2001:134:247–264.
- Skinner BF. The behavior of organisms. New York: Appleton-Century-Crofts Inc; 1938
- Stout EE, Beloozerova IN. Pyramidal tract neurons receptive to different forelimb joints act differently during locomotion. J Neurophysiol. 2012:107:1890–1903.
- Stout EE, Beloozerova IN. Differential responses of fast- and slow-conducting pyramidal tract neurons to changes in accuracy demands during locomotion. *J Physiol Lond*. 2013:591(Pt 10): 2647–2666.
- Strick PL, Kim CC. Input to primate motor cortex from posterior parietal cortex (area 5). I. Demonstration by retrograde transport. *Brain Res.* 1978:157(2):325–330.
- Sun HJ, Carey DP, Goodale MA. A mammalian model of optic flow utilization in the control of locomotion. *Exp Brain Res.* 1992:91: 171–175.
- Swadlow HA. Neocortical efferent neurons with very slowly conducting axons: strategies for reliable antidromic identification. J Neurosci Methods. 1998:79:131–141.
- Swadlow HA, Waxman SG, Rosene DL. Latency variability and the identification of antidromically activated units in mammalian brain. Exp Brain Res. 1978:32:439–443.
- Trendelenburg W. Untersuchungen uber reizlose vorubergehende Aussaltung am Zentralnervensystem. III. Die extermitaten Region der Grosshirninde. Pflugers Archiv. 1911:137:515–544.

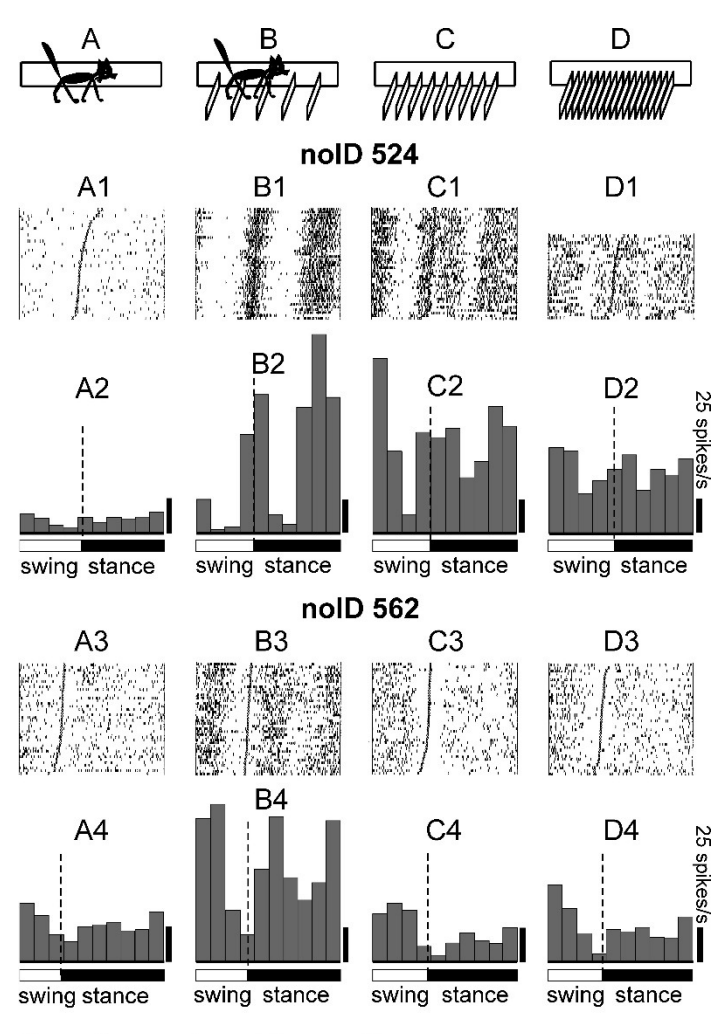
- Ungerleider LG, Mishkin M. Two cortical visual systems. In: Ingle DJ, Goodale MA, Mansfield RJW, editors. Analysis of visual behavior. Cambridge, MA: MIT Press; 1982
- Viala D, Viala G, Jordan M. Interneurones of the lumbar cord related to spontaneous locomotor activity in the rabbit. I. Rhythmically active interneurones. Exp Brain Res. 1991:84(1):177–186.
- Vicario DS, Martin JH, Ghez C. Specialized subregions in the cat motor cortex: a single unit analysis in the behaving animal. *Exp Brain Res.* 1983:51:351–367.
- Volgushev M, Nguyen CT, Iyer GS, Beloozerova IN. When cats need to see to step accurately? J Physiol Lond. 2022:660(1):75–94.
- Waters RS, Favorov O, Mori A, Asanuma H. Pattern of projection and physiological properties of cortico-cortical connections from the posterior bank of the ansate sulcus to the motor cortex, area 4 gamma, in the cat. Exp Brain Res. 1982:48(3):335–344.
- Wiesendanger M. The pyramidal tract. Its structure and function. Handb Behav Neurobiol. 1981:5:401–491.
- Wiesendanger R, Wiesendanger M, Ruegg DG. An anatomical investigation of the corticopontaine projection in the primate (Macaca fascicularis and Saimiri sciureus). II. The projection from frontal and parental association areas. *Neuroscience*. 1979:4: 747–765.
- Wong C, Lomber SG. Stable delay period representations in the posterior parietal cortex facilitate working-memory-guided obstacle negotiation. *Curr Biol.* 2019:29(1):70–80.e3.
- Wong C, Pearson KG, Lomber SG. Contributions of parietal cortex to the working memory of an obstacle acquired visually or tactilely in the locomoting cat. *Cereb Cortex*. 2018:28(9):3143–3158.
- Wong C, Wong G, Pearson KG, Lomber SG. Memory-guided stumbling correction in the hindlimb of quadrupeds relies on parietal area 5. Cereb Cortex. 2018:28(2):561–573.
- Wurtz RH. Neuronal mechanisms of visual stability. Vis Res. 2008:48: 2070–2089.
- Yumiya H, Ghez C. Specialized subregions in the cat motor cortex: anatomical demonstration of differential projections to rostral and caudal sectors. *Exp Brain Res.* 1984:53:259–276.
- Zubair HN, Beloozerova IN, Sun H, Marlinski V. Head movement during walking in the cat. Neuroscience. 2016:332:101–120.
- Zubair HN, Chu KMI, Johnson JL, Rivers TJ, Beloozerova IN. Gaze coordination with strides during walking in the cat. J Physiol Lond. 2019:597(21):5195–5229.



**Supplementary Figure 1.** Example responses of area 5 noID neurons to somatosensory and visual stimulation in the cat sitting with its head restrained.

**A:** Responses of noIDs #1158 and #1158a to flexion of the right shoulder.

**B:** Responses of noIDs #1596 and #1697 to approaching object (a cat toy).



**Supplementary Figure 2** 

Supplementary Figure 2. Example area 5 noID neurons during locomotion respond to the visual complexity of the walkway, not movement of limbs. These recordings were obtained in the course of a separate study, an abstract of which was published in Beloozerova and Sirota, 1992. The area of the suprasilvian gyrus from which the recordings were obtained is shown in Figure 1 in Beloozerova and Sirota, 2003.

**A - D:** Locomotion tasks. The cat walks on a flat surface (A) and then oversteps a series of barriers 70 mm tall that are placed either 25 cm apart (B), 12 cm apart (C) or 6 cm apart (D).

A1 - D1: Activity of noID #524 is presented as a raster of 40 (A1-C1) or 26 (D1) step cycles of each locomotion task. In the rasters, the duration of step cycles is normalized to 100%, and strides are rank-ordered according to the duration of the swing phase. The beginning of the stance phase in each stride is indicated by a cross.

**A2 - D2**: Corresponding histograms of the activity. Vertical bar on the right of each histogram equals 25 spikes/s.

**A3 - D3**: Activity of noID #562 is presented as raster of 40 step cycles of each locomotion task **A4 - D4**: Corresponding histograms of the activity.